Modelling the Antarctic Ice Sheet across the Mid Pleistocene Transition - Implications for Oldest Ice

Johannes Sutter[1,2], Hubertus Fischer[2], Klaus Grosfeld[1], Nanna B. Karlsson[1], Thomas Kleiner[1], Brice Van Liefferinge[3,5], and Olaf Eisen[1,4]

[1]Alfred Wegener Institute Helmholtz-Centre for Polar and Marine Research, 27568 Bremerhaven, Germany
[2]Climate and Environmental Physics, Physics Institute, and Oeschger Centre for Climate Change Research, University of Bern, Bern, Switzerland
[3]Laboratoire de Glaciologie, Université libre de Bruxelles, CP 160/03, Avenue F.D. Roosevelt 50, B-1050 Brussels, Belgium
[4]Department of Geosciences, University of Bremen, Bremen, Germany
[5]Norwegian Polar Institute Fram Centre, NO-9296, Tromsø, Norway

Correspondence: Johannes Sutter (johannes.sutter@awi.de)

Abstract. The international endeavour to retrieve a continuous ice core, which spans the middle Pleistocene climate transition ca. 1.2-0.9 Myr ago, encompasses a multitude of field and model-based pre-site surveys. We expand on the current efforts to locate a suitable drilling site for the oldest Antarctic ice core by means of 3D continental ice-sheetice sheet modelling. To this end, we present an ensemble of ice-sheetice sheet simulations spanning the last 2 Myr, and employing transient boundary conditions derived from climate modelling and climate proxy records. We discuss the imprinteffects of changing climate conditions, sea level and geothermal heat flux boundary conditions on the ice thickness and basal conditions around previously identified sites with continuous records of old icethe mass balance and ice dynamics of the Antaretic Ice Sheet. Our modelling results show a range of configurational ice-sheetice sheet changes across the middle Pleistocene transition, suggesting a potential shift of the West Antarctic Ice Sheet to a marine-based configuration. Despite the middle Pleistocene climate re-organisation and associated ice-dynamic changes, we identify several regions conducive to conditions maintaining 1.5 Myr (Million years) old ice, particularly around Dome Fuji, Dome C and Ridge B, which is in agreement withto previous studies. This finding strengthens the notion that continuous records with such old ice do exist in previously identified regions, while we are also providing a dynamic continental ice-sheetice sheet context.

1 Introduction

The middle Pleistocene transition (MPT) is characterised by a shift from obliquity driven climate cycles ($\sim$ 41.000 years , 41 kyr) to the signature sawtooth $\sim$ 100 kyr cycles typical for the late Pleistocene. The drivers behind the MPT are still under debate and touch on the basic understanding of the climate system. The absence of any clear disruptive change during the MPT in orbital forcing makes the transition especially puzzling. Several theories have been put forth, striving to explain the

enigmatic MPT (Raymo and Huybers, 2008). They include a shift in subglacial conditions underneath the Laurentide Ice Sheet (regolith hypothesis by Clark and Pollard (1998)), the inception of a large North American Ice Sheet (Bintanja and van de Wal, 2008) or marine East Antarctic Ice Sheet by Raymo et al. (2006), ice bedrock climate feedbacks (Abe-Ouchi et al., 2013), the buildup of large ice sheets between MIS24 and 22 identified by Elderfield et al. (2012), or the combination of changes of ice-sheetice sheet dynamics and the carbon cycle (Chalk et al., 2017). Ultimately, it seems likely that an interplay of the various proposed processes culminated in the MPT. To illuminate the potential role of these different processes and thus to solve one of the grand challenges of climate research, the recovery of a continuous ice core spanning at least beyond the MPT (in the following termed as "Oldest Ice") is crucial.

An expansion of the currently longest ice core record from the EPICA Dome C project (Jouzel et al., 2007) to and beyond the MPT, would provide the necessary atmospheric boundary conditions (i.e. atmospheric greenhouse gases and surface temperature) to revisit the current theories (Fischer et al., 2013). It would provide a direct record of global atmospheric CO_2 and CH_4 concentrations and local climate during the MPT and beyond. A transient record of CO_2 concentrations would provide a key piece of the puzzle in answering the question whether greenhouse gases were the main culprit behind the MPT, while proxies of climate conditions in Antarctica would illuminate the evolution of the Antarctic Ice Sheet leading to the MPT. However, retrieval of such an ice core is a challenging task, as a multitude of prerequisites must be met (Fischer et al., 2013; Fischer et al., 2013; Fischer et al., 2017) to recover an undisturbed ice core reaching more than a million years into the past (Fischer et al., 2013; Van Liefferinge and Pattyn, 2013; Parrenin et al., 2017). The European ice core communityIPICS-community (International Partnership in Ice Core Sciences) has identified athe most promising target for an Oldest Ice drill site to be close to a secondary dome in the vicinity of Dome C, usually referred to as "Little Dome C" (LDC) (Parrenin et al., 2017). Also, other potential locations are targeted around Dome Fuji. The selection of sites is motivated by a series of recent studies based both on radar observations of the internal ice-sheetice sheet stratigraphy and underlying bedrock topography (Young et al., 2017; Karlsson et al., 2018), local paleoclimate conditions (Cavitte et al., 2018), as well as 1D and 3D ice-flow modelling (Van Liefferinge et al., 2018; Parrenin et al., 2017; Passalacqua et al., 2017). These studies provide a detailed view on the regional properties such as ice flow, thermal conditions and bedrock topography, enabling a localized assessmentestimate of promising drill sites. The only component missing so far in the analysis is the transient, continental paleo ice-sheetice sheet dynamics perspective, which allows for the assessment of large-scale re-organizations of ice-sheetice sheet flow and geometry during glacial and interglacial cycles, their impact on divide migration, ice thickness changes along the East Antarctic ice divide and basal melt. There are many studies focussing on the transient evolutiondynamics of the Antarctic Ice Sheet (AIS) during specific climate episodes in the past such as the Last Interglacial (LIG) (Sutter et al., 2016; DeConto and Pollard, 2016) or the Last Glacial Maximum (LGM) (e.g. Golledge et al., 2014). However, so far only a few studies cover the waxing and waning of the AIS during the MPT (Pollard and DeConto, 2009; de Boer et al., 2014) or late Quaternary (Tigchelaar et al., 2018) in transient model simulations with an evolving climate forcing. We build on these efforts by carrying out ensemble simulations of the Antarctic Ice Sheet across the last 2 Myr to investigate the MPT and the effect of glacial-interglacial variations in ice thickness and basal meltingdynamics on potential Oldest Ice drill sites.

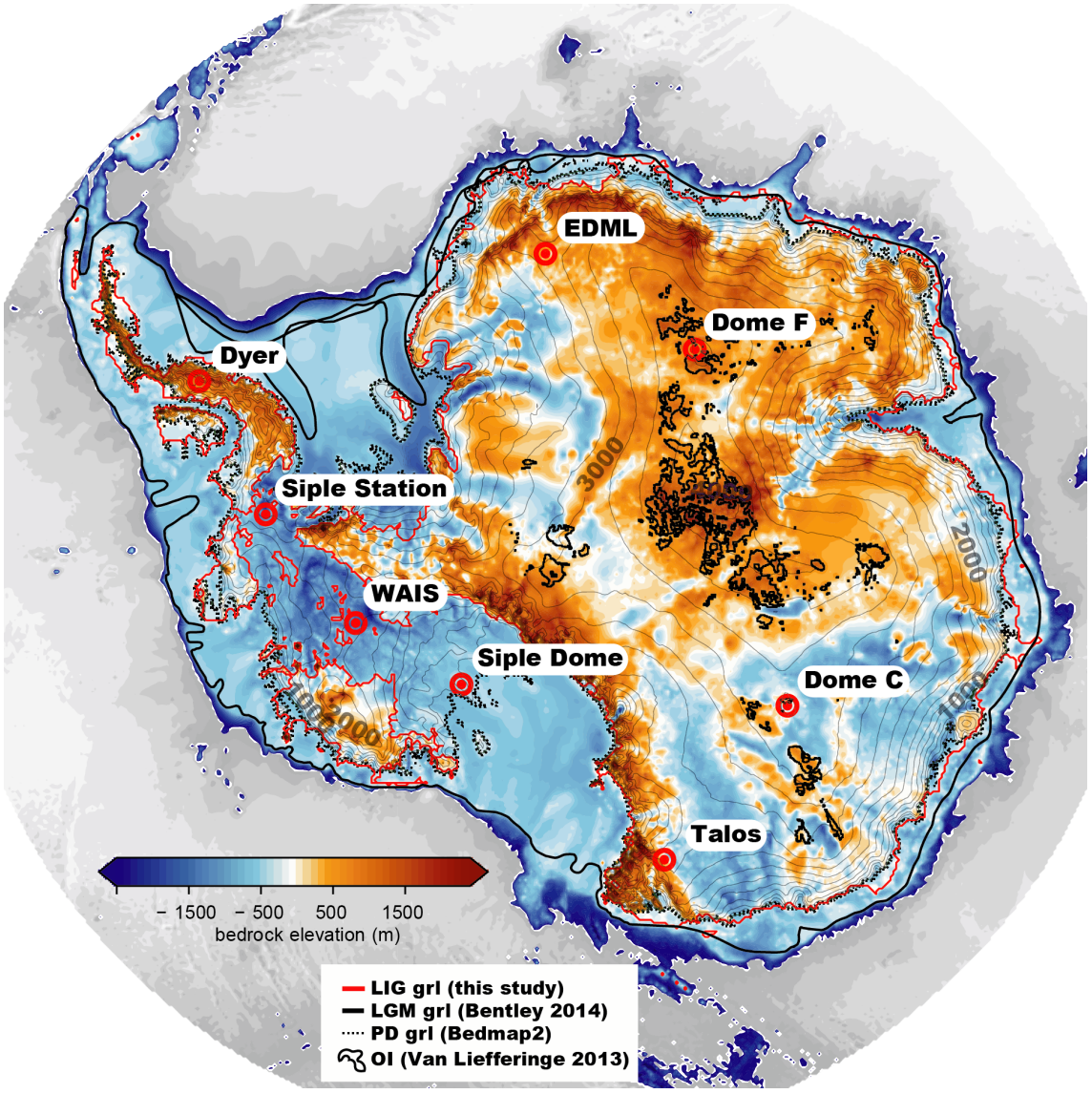

Figure 1. Antarctic bedrock topography overlain by surface contours (gray lines). The present day (PD) grounding line from BEDMAP2 (Fretwell et al., 2013) depicted by the dashed black line. Last Glacial Maximum (LGM) grounding line reconstruction from Bentley et al. (2014) (thick black lines) is compared to simulated grounding line retreat in one of the ensemble members for the Last Interglacial (LIG, red line). Regions previously identified as potentially viable sites for Oldest Ice (Van Liefferinge and Pattyn, 2013) are outlined by thick black lines. Eight ice core locations are highlighted, which are used as tuning targets with respect to ice core thickness and analysed in Figure 9 (West Antarctica) and 10 (East Antarctica), respectively.

2 Methods

2.1 Ice Sheet Model

We employ the 3D thermomechanical Parallel Ice Sheet Model (PISM) (Bueler and Brown, 2009; Winkelmann et al., 2011) in the hybrid shallow-ice/shallow-shelf~~shallow-shelf/shallow-ice~~ mode (SIA+SSA)~~(ssa+sia)~~ with a subgrid grounding line parameterisation (Gladstone et al., 2010; Feldmann et al., 2014) to allow for reversible grounding line migration despite using a relatively coarse resolution. Basal sliding is calculated with a pseudo-plastic sliding law (Schoof, 2010) in which the yield stress (τ_c) is determined by the pore water content and the strength of the sediment which is set by a linear piecewise function dependent on the ice-bedrock interface depth relative to sea level. The relevant parameter for this approach is introduced in PISM via the till-friction angle (see Winkelmann et al. (2011) eq. 12) which is scaled linearly between till_{min} and till_{max}, depending on the bedrock elevation (see Table 2). Through this heuristic parameterisation marine-based ice has a more slippery base as compared to ice above sea level, allowing for faster flowing marine outlet glaciers. The parameter space used here yields a basal friction coefficient (e.g. underneath Thwaites glacier) on the lower end compared to Yu et al. (2018). Since the simulations presented here span a long time period~~frame~~ (of 2 Myr~~2 MA~~), we abstain from the derivation of basal friction by inversion (optimization problem) as we want to prevent over-tuning of present-day flow patterns. All simulations are carried out on a 16x16 km^2 grid and 81 vertical levels with refined resolution near the base (≈ 18 m at the ice-bedrock interface). The grid resolution resolves the major ice streams while allowing for reasonable computation times (ca. 100 model years per processor hour on 144 cores, i.e. ca 5-7 days for 2 Myr depending on the supercomputer load), yet small outlet glaciers such as in the Antarctic Peninsula cannot be simulated adequately on this resolution.

The initial topography used for the simulations consists of a 200 kyr thermal spinup of the BEDMAP2 (Fretwell et al., 2013, see Figure 1) data set (present day steady state simulation with fixed ice-sheet~~ice sheet~~ geometry), refined around LDC and Dome Fuji by the new radar derived topographies published in Young et al. (2017) and Karlsson et al. (2018). As basal heat flux is crucial for the existence of 1.5 Myr old ice (Fischer et al., 2013; Van Liefferinge and Pattyn, 2013) as well as for ice dynamics, especially in the interior of the ice sheet (Larour et al., 2012), we consider four different geothermal heat flux (GHF) data sets (Shapiro and Ritzwoller, 2004; Purucker, 2013; An et al., 2015; Martos et al., 2017) in our simulations to account for uncertainties in GHF and to illustrate their impact on ice dynamics and potential Oldest Ice candidate sites.

Sea level plays an important role in the stability of marine ice sheets as it affects the position of the grounding line via the floatation criterion. We employ three different sea level reconstructions (see section 2.3) to account for different glaciation patterns in the northern hemisphere and different sea level highstands in interglacials. PISM does not account for self-gravitational effects yet, which can have a stabilising effect on the ice sheet locally in interglacials (e.g. Konrad et al., 2014). Ice-shelf melt rates are calculated based on the parameterisation in Beckmann and Goosse (2003) (eq. 1), with a square dependency on the temperature difference between the pressure dependent freezing point and the ambient ocean temperature as used in e.g. Pollard

and DeConto (2012),

$$M = m_b 0.005 \frac{\rho_w c_{pw}}{L_i \rho_i \gamma_T} |(T^{3D}_{ocean} - T_f)|(T^{3D}_{ocean} - T_f) \quad (1)$$

where M is the melt rate in m/s, m_b is a scaling factor, ρ_w and ρ_i are ocean water and ice-shelf density, respectively, c_{pw} is ocean water heat capacitiy, γ_T heat transfer coefficient, L_i latent heat, T_f freezing point at depth of ice and T^{3D}_{ocean} ambient ocean temperature. The ambient ocean temperature T^{3D}_{ocean} is derived from simple extrapolation of the 3D ocean temperature into the ice-shelf cavity. Recently, there have been developments towards more realistic representations of basal shelf melt in standalone continental ice-sheetice sheet models, incorporating sub-shelf ocean circulation (e.g. Reese et al., 2018; Lazeroms et al., 2018) which improve the representation of basal ice-shelf melt rates, but they have not been included in this study. To better match present day observed sub ice-shelf melt rates (Rignot et al., 2013; Depoorter et al., 2013), we had to multiplylinearly scale the computed present day melt rates in the Amundsen and Bellinghausen Sea by a factor of $m_b = 10$, around the Antarctic Peninsula by 5, and underneath the Filchner Ice-Shelf by a factor of 1.5. Shelf melt rates adjacent to Wilkes, Terre Adelie and George V Land in East Antarctica are also multiplied by factor of 10 in a subset of the simulations. These scaling factors are kept constant throughout the paleo simulations. Ice-shelf calving and therefore the dynamic calving front is derived via two heuristic calving parameterisations: 1. thickness calving (cH) sets a minimum spatially uniform ice thickness (75 m or 150 m) at the calving front. If the ice thickness drops below this threshold, ice in the respective grid node is purged; 2. independently of 1. we additionally employ Eigencalving (cE), which calculates a calving rate from the ice-shelf strain rates (Albrecht and Levermann, 2014). Both calving parameterisations are active simultaneously throughout the simulations.

2.2 Climate Forcing

To adequately capture continental ice-sheetice sheet dynamics on multi-millenniallong timescales (i.e. millennia and more), in principle, a coupled modelling approach is required which resolvesto resolve climate-ice-sheetice sheet interactions is required. First efforts to tackle multi-millennial timescales via a fully coupled modelling approach are promising and currently being developed (e.g. Ganopolski and Brovkin, 2017). However, coupled climate-ice-sheetice sheet models which resolve ice-shelf–ocean interactions are mostly limited to applications on the centennial time scale due to computational limitations. To bridge this shortcoming, we construct a transient climate forcing over the last 2 Myr by expanding time-slice snapshots from the Earth system model (ESM) COSMOS (Lunt et al., 2013) with a climate indexthe glacial index method as applied in Sutter et al. (2016). The climate snapshots are based on Pliocene (Stepanek and Lohmann, 2012), LIG (Pfeiffer and Lohmann, 2016), LGM and Pre-Industrial orbital, atmospheric and topographic conditions. For each climate snapshot, anomaly fields with respect to the pre-industrial control run are calculated and added to a mean Antarctic climatology (1979-2011), derived from the regional climate model RACMO (van Wessem et al., 2014), or the extrapolated World Ocean Atlas 2009 (Locarnini et al., 2010) to provide the climate forcing for the individual climate epoch. The intermediate climate states between the snapshots are calculated by interpolating the anomaly fields with a climate indexglacial index approach, utilizing either of two climateglacial indices (see Figure 6 middle panel) derived from the Dome C deuterium record from Jouzel et al. (2007) which is expanded to the last 2 Myr by a transfer function (Michel et al., 2016) using the benthic oxygen isotope stackmarine sediment core from

Lisiecki and Raymo (2005) (LR04) or the global surface temperature data set from Snyder (2016). To obtain an "Antarctic" surface temperature record from the far field benthic oxygen isotope stack, the LR04 isotope values are scaled via:

$$LR04_T = -(LR04 - \overline{LR04_{810}})\frac{\sigma(EDC2007)}{\sigma(LR04_{810})} + \overline{EDC2007} - 55K \tag{2}$$

$LR04_T$ is the new surface temperature record, $LR04$ is the benthic isotope stack data (time corrected to match the AICC2012 time scale (Bazin et al., 2013; Veres et al., 2013)) and $\overline{LR04_{810}}$ is the mean LR04 isotope data for the last 810 kyr, standard deviations of the EDC and $LR04_{810}$ record are denoted by $\sigma(EDC2007)$ and $\sigma(LR04_{810})$, respectively, mean Dome C surface temperature record is denoted by $\overline{EDC2007}$. The forcing variables (surface temperature T_s, ocean temperature T_o) can then be calculated at every grid point in time by:

$$T_s^{i,j}(t) = T_{spd}^{i,j} + \sum_{x=\mathrm{ig,g,p}} \omega_x(t)\Delta T_s{}_x^{i,j} \tag{3}$$

$$T_o^{i,j,z}(t) = T_{opd}^{i,j,z} + \sum_{x=\mathrm{ig,g,p}} \omega_x(t)\Delta T_o{}_x^{i,j,z} \tag{4}$$

where indices i,j denotes the grid point, z denotes the depth of the ice ocean interface at grid point (i,j), $T_s^{i,j}(t)$ is the surface temperature at grid point i,j at time t, $T_{spd}^{i,j}$ is the surface temperature at present day (mean climatology from 1979-2016), $\Delta T_{s_{ig}}^{i,j}$, $\Delta T_{s_g}^{i,j}$ and $\Delta T_{s_p}^{i,j}$, are the climate anomalies for the LIG, the LGM and the Pliocene, respectively. Ocean temperatures are derived in the same way (eq. 4). The linear scaling ~~factors~~ $\omega_x(t)$ ~~are~~ derived from the climate index~~glacial index~~ (CI) ~~which~~ interpolates the climate forcing at any given time between the respective climate states. The scaling $\omega_x(t)$ is computed by :

$$\omega_g(t) = 1.0 - \frac{min(\mathrm{CI}, \mathrm{CI_{pd}})}{\mathrm{CI_{pd}}}) \begin{cases} 1.0 \text{ for } \mathrm{CI} = 0.0 \\ 0.0 - 1.0 \text{ for } 0.0 < \mathrm{CI} < \mathrm{CI_{pd}} \\ 0.0 \text{ for } \mathrm{CI} \geqslant \mathrm{CI_{pd}} \end{cases} \tag{5}$$

$$\omega_{ig}(t) = \frac{(max(\mathrm{CI}, \mathrm{CI_{pd}}) - \mathrm{CI_{pd}})}{(1.0 - \mathrm{CI_{pd}})} \begin{cases} 1.0 \text{ for } \mathrm{CI} = 1 \\ 0.0 - 1.0 \text{ for } \mathrm{CI_{pd}} \leqslant \mathrm{CI} \leqslant 1.0 \\ 0.0 \text{ for } \mathrm{CI} \leqslant \mathrm{CI_{pd}} \end{cases} \tag{6}$$

$$\omega_p(t) = \frac{(max(\mathrm{CI}, 1.0) - 1.0)}{(\mathrm{CI_p} - 1.0)} \begin{cases} 1.0 \text{ for } \mathrm{CI} = \mathrm{CI_{max}} \\ 0.0 - 1.0 \text{ for } 1.0 \leqslant \mathrm{CI} \leqslant \mathrm{CI_{pd}} \\ 0.0 \text{ for } \mathrm{CI} \leqslant 1.0 \end{cases} \tag{7}$$

where the subscripts g, ig and p stand for Glacial, Interglacial and Pliocene respectively and CI_{pd} refers to the present day climate index~~glacial index~~. The respective values of the climate indices are $\mathrm{CI}_{lgm} = 0.0$, $\mathrm{CI}_{pd} = 0.70$, $\mathrm{CI}_{lig} = 1.0, CI_p = 1.13$.

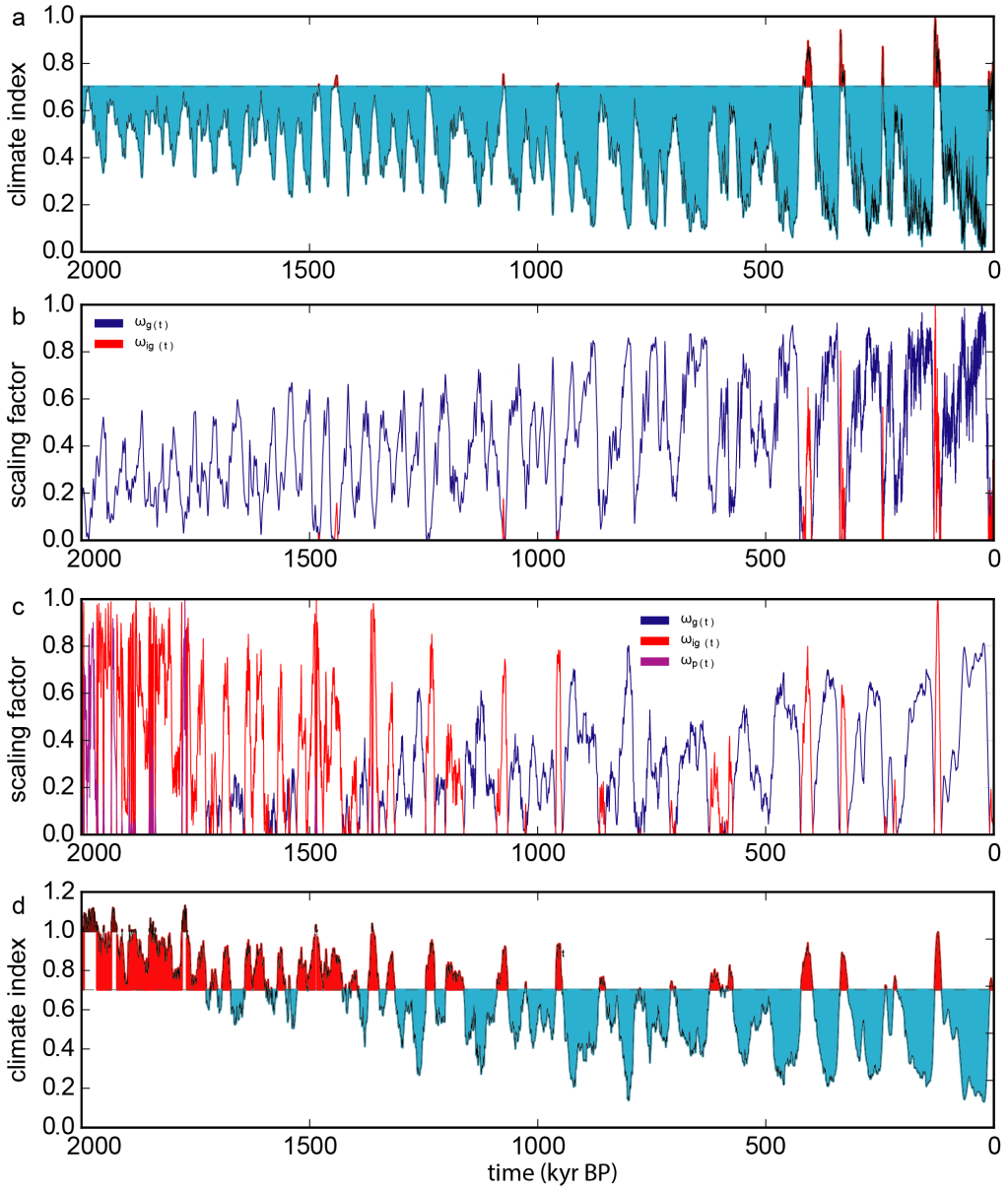

Figure 2. Climate index~~glacial index~~ derived from Dome C deuterium record a) and corresponding scaling factors ω_x in b). Times colder than present are shaded in cyan and times warmer than present in red. d) same as as a) but for the climate index~~glacial index~~ derived from the Snyder global surface temperature record and scaling factors ω_x in c). Times warmer than the Last Interglacial are shaded in dark red. The lines in b) and c) vanish when scaling factors are zero.

The climate index is normalized with respect to the warmest climate period in the Dome C temperature record, therefore the LIG has index 1.0 in ensemble B1 and B2. The climate is linearly scaled between present day and LIG if the climate index surpasses the mean present day climate index CI_{pd}, and between LIG and the Pliocene if the index is larger than 1.0. The major difference between the two glacial indices is the warmer overall climate state recorded in Snyder (2016) before the MPT (see Figure 2 b). The present day forcing derived from van Wessem et al. (2014) matches the present day climatology in Antarctica (compared to in-situ measurements) very well, with biases in the high Antarctic plateaus of less than 5%.

We apply a temperature dependent scaling of precipitation (P), using a scaling factor (percent precipitation change per degree Celsius) of α_P of 3 and 5 $\%$, respectively, motivated by central East Antarctic paleo precipitation changes (Frieler et al., 2015; Werner et al., 2018):

$$P(t) = P_{pd} + (T^{i,j}_{spd} - T^{i,j}_{s}(t))\alpha_P. \quad (8)$$

The precipitation is linearly dependent on the temperature anomaly with respect to present day temperature. Note that this scaling ~~but~~ underestimates~~underestimating~~ the sensitivity of coastal mass balance to temperature changes.

In this standalone approach, the ~~Antarctic Ice Sheet (~~AIS is responding to the external forcing, thus no feedbacks are acting between the ice sheet and the climate system. However, the climate index~~glacial index~~ approach implicitly incorporates the integrated climate response to changes in orbital configuration and atmospheric CO_2 archived in the Dome C (Jouzel et al., 2007), the marine sediment core (Lisiecki and Raymo, 2005) or the global surface air~~air~~ temperature (Snyder, 2016) record. This allows to investigate the dynamical response of the AIS to a shifting climate regime across the MPT, with the caveat, that ice-sheet~~ice sheet~~ –climate interactions which are not included in the GCM time slice approach might have also played a significant role in the evolution of the AIS during the MPT ~~transition~~.

2.3 Model ensemble approach

We choose a model ensemble approach, to address the multitude of uncertainties regarding the paleoclimate state during the last 2 million years, the applied boundary conditions and the physics of ice flow ~~,we choose a model ensemble approach~~. The aim of the ensemble design (Figure 3) is to investigate the impact of different climate forcings, the response of the AIS to different geothermal heat flux signatures (Figure 4) and the impact of sea level ~~(Figure 6, bottom panel)~~ on the transient configuration of marine ice sheets. Ultimately, different manifestations of ice-sheet~~ice sheet~~ flow and climate response are investigated via a set of ice-sheet~~ice sheet~~ model parameterisations. The model parameters are pre-selected in equilibrium simulations under present day forcing (1979–2011 climatology from van Wessem et al. (2014) and World Ocean Atlas (Locarnini et al., 2010) ocean temperatures) trying to fit the current sea level equivalent ice-sheet~~ice sheet~~ volume, geometry, ice flow, ice thickness at selected ice core locations (Figure 1), as well as the Antarctic sea level contribution during the last two glacial cycles. The ensemble is built around two main branches of ensemble runs consisting of a set of boundary conditions (Table 1) and ice-sheet~~ice sheet~~ model parameterisations (Table 2).

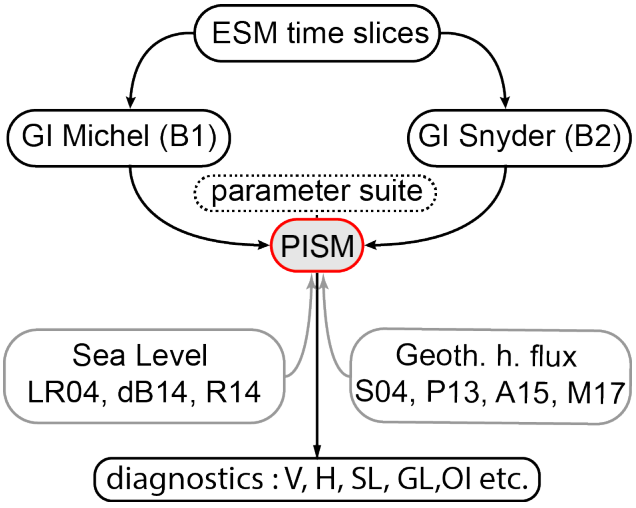

Figure 3. Schematic flow chart of the model ensemble. The ice-sheet~~ice sheet~~ model (PISM) is forced via the transient forcing derived by linear interpolation with glacial indices from Michel et al. (2016) and Snyder (2016) forming ensemble branch B1 and B2. Prescribed input data consist of sea level (SL) data and geothermal heat flux (GHF) data sets. Both ensemble B1 and B2 are constructed with twelve different forcing combinations (three SL data sets and four geothermal heat flux fields). The parameter suite is derived from sensitivity studies in which the present day Antarctic Ice Sheet and its sea level contribution during the last two glacial cycles were the main tuning targets.

Table 1. Available choices of selected forcing fields for the model ensemble. B1 and B2 stand for the two glacial indices derived from Michel et al. (2016) and Snyder (2016); SL data from Lisiecki and Raymo (2005) (LR05), de Boer et al. (2014) (dB14), and Rohling et al. (2014) (R14); GHF data from Shapiro and Ritzwoller (2004) (S04), Purucker (2013) (P13), An et al. (2015) (A15), and Martos et al. (2017) (M17).

Forcing	GI	SL	GHF
Data	B1, B2	LR05, dB14, R14	S04, P13, A15, M17

In the first ensemble branch (B1) the climate index~~glacial index~~ is derived from an extrapolation of the EPICA Dome C temperature record (Jouzel et al., 2007) via correlation to the Lisiecki and Raymo (2005) time series to span the last two million years (Michel et al., 2016). In the second branch (B2) the climate index~~glacial index~~ is derived from the global ~~air~~ temperature record in Snyder (2016). Major differences between 2–0.9 Myr BP can be identified in the two resulting glacial indices. B2 exhibits much warmer climate conditions between 2–1.2 Myr ago. The warmest climate state in B1 is the ESM time slice centred in the LIG (MIS5) (Pfeiffer and Lohmann, 2016) while in B2 the interglacials between 2 and 1.7 Myr BP are the warmest, represented by a middle Pliocene climate time slice (Stepanek and Lohmann, 2012) (see Figure 2).We explore two main parameter sets (P1 and P2) highlighted in Table 2. While we do take into account all sea level variations for ensemble B1, we only look at the sea level forcing derived from Lisiecki and Raymo (2005) (LR05) in ensemble B2. We also experimented with other parameter choices based on Table 2 (VP) but do not cover~~ing~~ all individual forcing sets for these, thus they are not

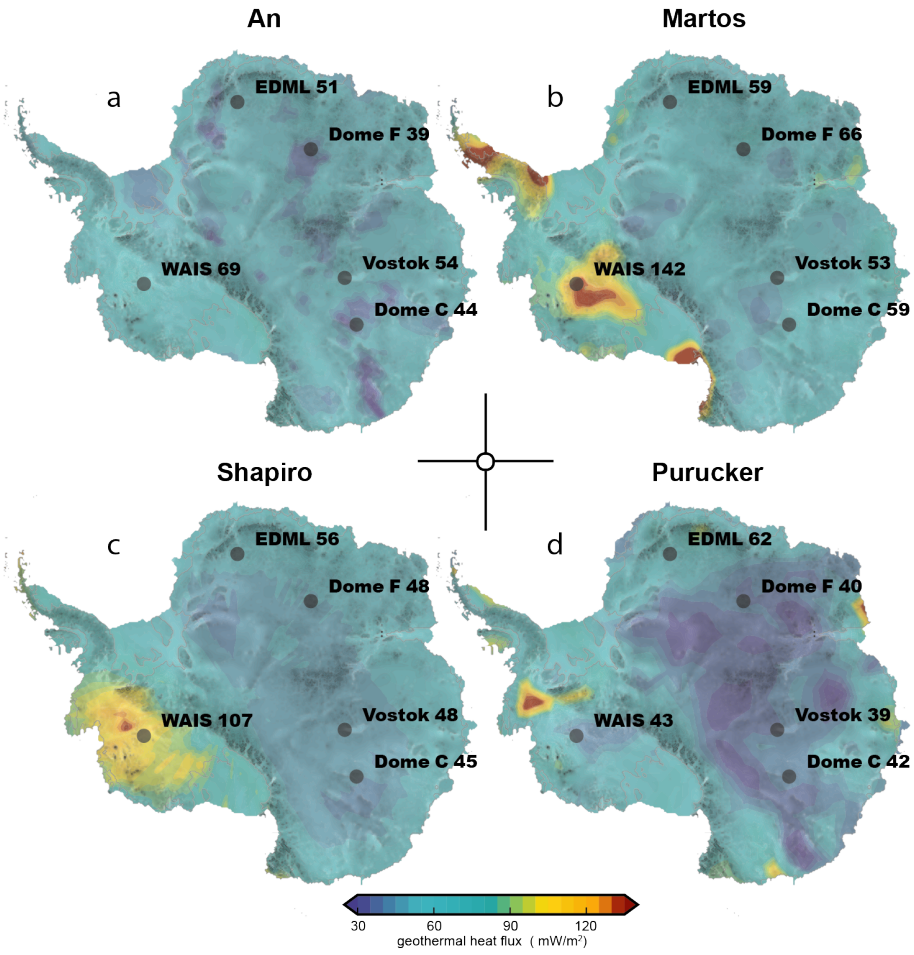

Figure 4. The four panels illustrate the four GHF input data sets (Shapiro and Ritzwoller, 2004; Purucker, 2013; An et al., 2015; Martos et al., 2017) used in this study. As a reference the rounded GHF (in $\mathrm{mW/m2}$) at selected ice core locations is provided.

discussed in this study. In total we carried out 186 individual simulations. The ensemble members discussed in this manuscript consist of 8 experiments for each ensemble B1 and B2 with sea level forcing from LR05.

3 Results & Discussion

The main objective of this work is to assess the existence of 1.5 Myr old ice along the East Antarctic ice divide. We simulate the evolution of the AIS~~ice dynamics~~ throughout the last 2 Myr, focussing on ice volume changes specifically across the MPT (see Figure 5 and 6), as well as on ice-sheet~~ice sheet~~ configurations in glacials (focussing on marine isotope stage 2) and interglacials (with a focus on marine isotope stage 11 and 5, see Figure 7 and 8). We further investigate ice thickness changes

Table 2. Selected ISM parameters for the model ensemble. First and second line show the main parameter sets used in the ensemble (P1 and P2). The third line lists additional parameters tested but not further used and discussed in this study (VP). cH stands for thickness calving limit (in meter), cE is a parameter in the Eigencalving equation; sia_e and ssa_e stand for the so called SIA and SSA "enhancement factors", $till_{min}$ and $till_{max}$ modify basal friction in the sliding law. γ_{EAIS} is a dimensionless scaling factor for basal shelf melt for selected East Antarctic ice-shelf regions (George V Land, Wilkes Land).

Parameter	sia_e	ssa_e	cH (m)	cE	$till_{min}$	$till_{max}$	γ_{EAIS}
P1	1.0	0.55	**75**	$1 \cdot 10^{17}$	5	30	**10**
P2	1.0	0.55	**150**	$1 \cdot 10^{17}$	5	30	**1**
VP	1.6 ; 1.7 ; 2.0	1.0	100	$1{\cdot}10^{18}$	10	40	5-20

at ice core locations in West and East Antarctica (see Figure 9 and 10). We conclude with a map of promising sites providing suitable conditions for an Oldest Ice ice core around Dome Fuji, Dome C and Ridge B, following the approach of Fischer et al. (2013) and Van Liefferinge and Pattyn (2013) (Figure 11).

3.1 Antarctic ice volume changes

We divide our discussion of the evolution of the AIS volume into three time frames: 1. pre-MPT (2 – 1.2 Myr BP), MPT (1.2 – 0.9 Myr BP), and post-MPT (0.8 – 0 Myr BP). To put our results into perspective, we compare them to two published transient ice-sheet~~ice sheet~~ model studies which cover the time interval considered here (Pollard and DeConto (2009) and de Boer et al. (2014)) as well as Tigchelaar et al. (2018), which spans the last 0.8 Myr. Figures 5 and 6 depict the transient evolution of AIS volume as simulated by the whole ensemble and a representative subset of our model ensemble in comparison to Pollard and DeConto (2009), de Boer et al. (2014) and Tigchelaar et al. (2018) and with respect to different choices of GHF and climate index~~glacial index~~. In Figure 6, we present two clusters of the model ensemble from branch B1 (ice/marine sediment core climate index~~glacial index~~) and the branch B2 (surface air~~global air~~ temperature climate index~~glacial index~~). Depicted are three simulations from both B1 and B2 with two ~~identical~~ model parameterisations (P1 and P2, respectively, see Table 2) using three different GHF data sets (Shapiro and Ritzwoller, 2004; Purucker, 2013; Martos et al., 2017).

3.1.1 Pre-MPT Antarctic ~~Ice-Sheet~~~~Ice Sheet~~ ~~evolution~~~~dynamics~~

Simulated ice volume changes before the MPT are characterised by a strong obliquity (≈ 41 kyr) cycle resembling the climate index~~glacial index~~ forcing which is formed by the integrated planetary response to orbital variations. The two clusters in the upper panel of Figure 6 show an ~~a present day~~ ice-sheet~~ice sheet~~ configuration similar to present day (B1-branch) and a strong Interglacial configuration (B2-branch) in which the West Antarctic Ice Sheet (WAIS) has collapsed. Note that most of the ensemble members do not allow a significantly increased glaciation as encountered during the last 800 kyr. The increase in glacial AIS volume ~~increase~~ during the pre-MPT phase is limited to less than 2-4 m sea level equivalent ice volume throughout

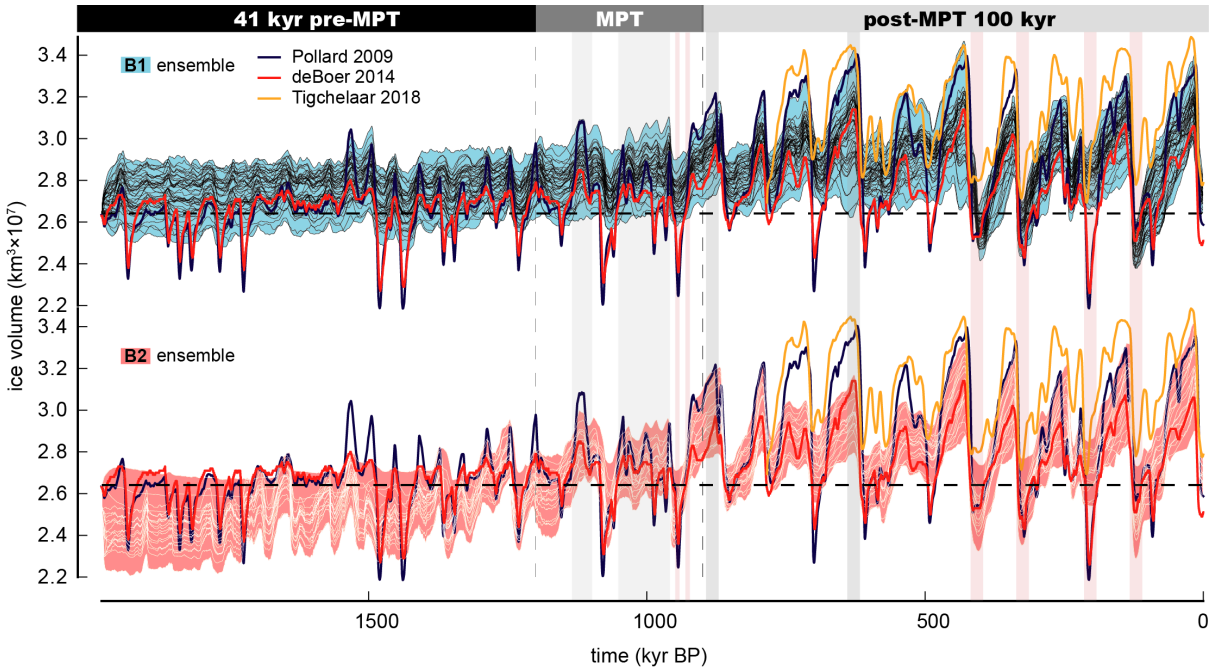

Figure 5. Antarctic ice volume as simulated in the full model ensemble (excluding simulations with either present day ice volume larger than $2.8 \cdot 10^7$ km^3 or Last Glacial Maximum ice-sheet~~ice sheet~~ volume smaller than $3.0 \cdot 10^7$ km^3). The horizontal black dashed line denotes present day ice volume derived from BEDMAP2 (Fretwell et al., 2013).

the model ensemble. Variability in the B2-branch (red) is higher than in B1 (blue), due to~~resembling~~ the waxing and waning of the marine WAIS and stronger Glacial–Interglacial surface mass balance variability. Ice volume in the B1-branch is predominantly driven by surface mass balance and sea level. The comparison to Pollard and DeConto (2009) and de Boer et al. (2014) illustrates the imprint of the different forcing approaches. While Pollard and DeConto (2009) and de Boer et al. (2014) both follow a combined approach using far field proxies as well as austral summer insolation (80°S), we construct a transient climate forcing by combining Antarctic Earth System Model (ESM) snapshots from the Pliocene, LIG and LGM with two glacial indices derived from far field proxies. One of the main differences in our approach and the forcing applied in Pollard and DeConto (2009) and de Boer et al. (2014) is the handling of basal melting underneath the ice shelves. This forcing component arguably exerts the strongest influence on grounding line migration of the AIS in interglacials. Our calculation of basal melt rates is very similar to de Boer et al. (2014), with smaller~~lower~~ differences between assumed peak interglacial and present day uniform ocean temperature. Peak interglacial ocean temperatures for ensemble B1 are approximately 2°C (Last Interglacial) warmer than present day and 3°C warmer (Pliocene) in B2 (3.7°C in de Boer et al. (2014), with $-1.7°$ circum-antarctic ocean temperatures at present day and $+2°$ at peak interglacial). Additionally, we increase the sensitivity of the basal melt rate to ocean temperature changes in certain ocean basins (see method section). Pollard and DeConto (2009) prescribe basal melt rates directly, scaling them via the far field benthic isotope record (Lisiecki and Raymo, 2005) and austral summer insolation.

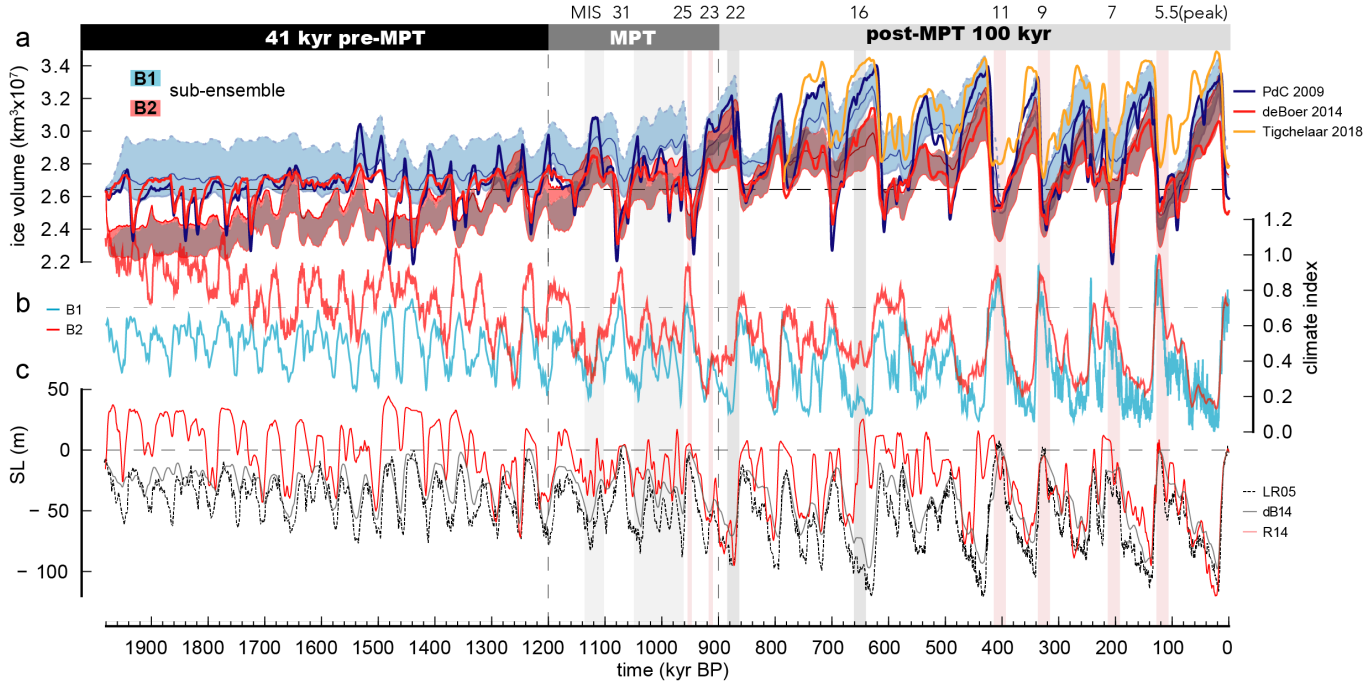

Figure 6. Panel a) depicts the ice volume evolution of a subset of the model ensemble. Blue and light blue curves depict ensemble branch B1 with parameter set P2 (see Table 2) and sea level forcing LR04. Geothermal heat flux depicted with blue line (Shapiro and Ritzwoller, 2004) upper light blue dashed line (Purucker, 2013) and lower light blue line (Martos et al., 2017). The red curves show B2 with parameter set P1 and using the climate index~~glacial index~~ from Snyder (2016). Red line (Shapiro and Ritzwoller, 2004), dashed maroon line (Martos et al., 2017), maroon line (Purucker, 2013)). The simulated ice volume from Pollard and DeConto (2009); de Boer et al. (2014); Tigchelaar et al. (2018) are shown for comparison (black, gray and black dashed line). The middle panel shows the climate index~~glacial index~~ used in B1(dark grey) and B2 (light gray) with the horizontal gray dashed line depicting the average Holocene index. The lower panel shows the sea level reconstructions used in the model ensembles ((Lisiecki and Raymo, 2005, LR04), (de Boer et al., 2014, dB14), (Rohling et al., 2014, R14)).

Ultimately, this scaling leads to larger bulk ice-shelf melt rates and smaller melt rates close to the grounding line compared to the ones calculated in our approach. Overall, this leads to a more muted ice-loss response to warmer interglacial conditions during the pre-MPT in our ensemble and a generally lower variability in ice volume (sea level equivalent of ca. $4-8$ m), while the growth and retreat phases are more or less synchronous to the variations in Pollard and DeConto (2009) and de Boer et al. (2014). Interestingly, the differences in interglacial AIS volume between the three studies are largest in pre-MPT times, while they are rather similar for the last four interglacials (see Figure 6). Evidently, the strongest interglacial AIS retreat is found in MIS7 for both Pollard and DeConto (2009) and de Boer et al. (2014), while in our ensemble it is MIS11 and MIS5, with MIS5 producing a slightly stronger response. A coherent result of~~One main similarity between~~ our study and the results from

Pollard and DeConto (2009) and de Boer et al. (2014) is that the East Antarctic Ice Sheet (EAIS) margins are relatively stable throughout the pre-MPT.

3.1.2 MPT Antarctic Ice-Sheet evolution~~dynamics~~

Commonly, the onset of the MPT is put at 1.2 Myr BP and the MPT ends about 0.9 Myr BP culminating in ~~the~~ extended cold conditions between marine isotope stages 24 and 22 (ca. 940-880 kyr BP). Two pronounced interglacials (MIS31 and MIS25) and several "colder-than-present" interglacials~~"lukewarm"~~ ~~events~~ (between 1050 kyr and 950 kyr BP) separated by moderate glacial conditions throughout the MPT can be identified in the climate index~~glacial index~~ forcing (Figure 6 panel b). The AIS response during the MPT is dominated by two proto-glacial states between 1.1 – 1.0 Myr BP separated by interglacial MIS31, which can be interpreted as a first expression of a 100 kyr cycle. However, obliquity pacing still dominates ice ice volume changes~~dynamics~~ at this stage. The second proto-glacial state after MIS31 is interupted by MIS25 followed by an extended cold period, allowing for the formation of marine ice sheets in the Weddell and Ross Seas similar to what is observed during late Quaternary glacials, marking the end of the MPT and the onset of unperturbed 80-120 kyr cycles in AIS volume. Our ice-sheet~~ice sheet~~ model results are in line with the notion of a 900-kyr event by Elderfield et al. (2012), which is centred around MIS25-22, manifesting itself in a qualitative difference in the formation of glacials: a long build up phase ended by a sharp decline of the ice volume into interglacials (late Quaternary sawtooth pattern) during the last 800 kyr and a more symmetric glaciation/deglaciation before the MPT. This finding is robust across all tested sea level forcing data sets. We find no evidence of large changes in the EAIS margin during the MPT as hypothesized by~~as in~~ Raymo et al. (2006), where a transition from a mostly land based EAIS to a marine EAIS similar to todays configuration is proposed. However, most simulations from B2, which include warm Pliocene climate conditions, show a major re-organisation of West Antarctica into a "present day" ice-sheet~~ice sheet~~ configuration at the end of the MPT (see Figure 9). This might represent a West Antarctic analogue~~pendant~~ to the theory that the EAIS transitioned to a marine configuration during the MPT (Raymo et al., 2006), which does not require significant changes in the EAIS margin during the MPT. Such a configurational WAIS-shift would potentially implicate strong climate feedback mechanisms due to the formation of an ocean gateway between the Weddell, Ross and Amundsen Sea (Sutter et al., 2016) affecting climate dynamics across the MPT. This transition is not simulated in B1 and calls for a more crucial analysis outside the scope of this publication, e.g. incorporating a fully coupled ESM with a dynamical ice-sheet~~ice sheet~~ component. Accordingly, the climate state in B1 does not allow a waxing and waning of the WAIS for pre-MPT interglacial conditions. We note, that other modelling studies either focussing on warmer Pliocene stages (DeConto and Pollard, 2016) or regional sensitivity studies (Mengel and Levermann, 2014) show large scale retreat of the grounding line into the Wilkes and Aurora subglacial basins, therefore a potential re-organization of the EAIS across the MPT cannot be excluded using all model experiments. The end of the MPT is marked by a pronounced glacial state at MIS 22 akin to the Last Glacial Maximum reflecting a strong growth of the AIS at the end of the MPT. This result is robust across all ensemble members for both branch B1 and B2. It is interesting to note that the glaciations in the MPT interval become progressively stronger and reach a full late Quaternary glaciation state in MIS 22.

3.1.3 Post-MPT Antarctic Ice-Sheet ~~evolution~~dynamics

The simulated Quaternary AIS volume evolution can be roughly divided into two parts, the first spanning the window from 900 kyr BP to 420 kyr BP (MIS11) and the second from MIS11 to today. After MIS11, ice volume variability increases with smaller interglacial and bigger glacial ice sheets compared to the preceeding 500 kyr. This pattern mostly reflects the stronger interglacial atmospheric and ocean temperature forcing from MIS11 onwards. MIS11 is the first late Quaternary interglacial in which the WAIS recedes to a land based ice-sheet~~ice sheet~~ configuration in B1 with the second major interglacial being MIS5e. The ensemble mean sea level contribution in MIS5e amounts to $\approx 2.5 - 3$ m with a full ensemble range between 1 and 4.5 m (see Figure 8). Glacial ice volume in the late Quaternary grows by ca. -8 to -10 m sea level equivalent ice volume (see Figure

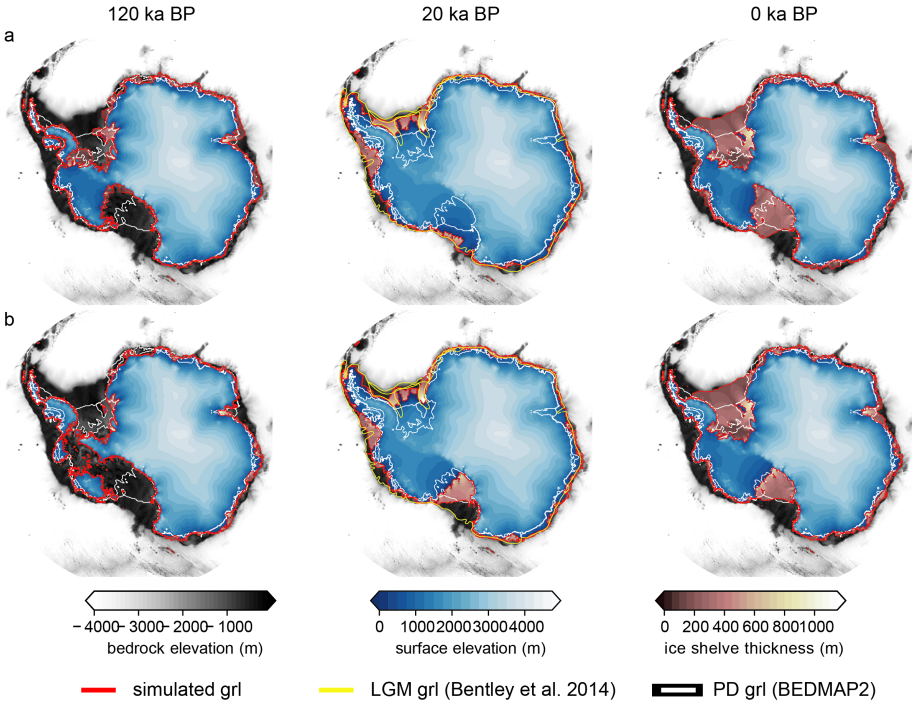

Figure 7. Panel a/b illustrate simulated ice-sheet~~ice sheet~~ configurations for the LIG, LGM and PD, respectively. Both simulations are carried out with forcing B1, using a different ice thickness calving limit (a: cH=75 m, b: cH=150 m). Reconstructed grounding line positions for the LGM (Bentley et al., 2014) are depicted in yellow. Both grounding line and ice-shelf front from BEDMAP2 (Fretwell et al., 2013) are depicted in white.

8) with strongest glacials represented by MIS16 and 2. In general, the glacial extent of the AIS matches reconstructed LGM grounding margins rather well, with the notable exception of the Ammundsen and Bellinghausen sea sectors. In this region, the ocean forcing seems to be too warm to allow for an advance of the ice margin to the continental shelf edge in the model. LGM ice growth in the whole ensemble is strongly dependent on the SIA enhancement factor sia_e, with values larger than 1.5 leading to an underestimation of ice thickness, albeit not necessarily ice extent. In the Ross Sea, ice thickness calving exerts

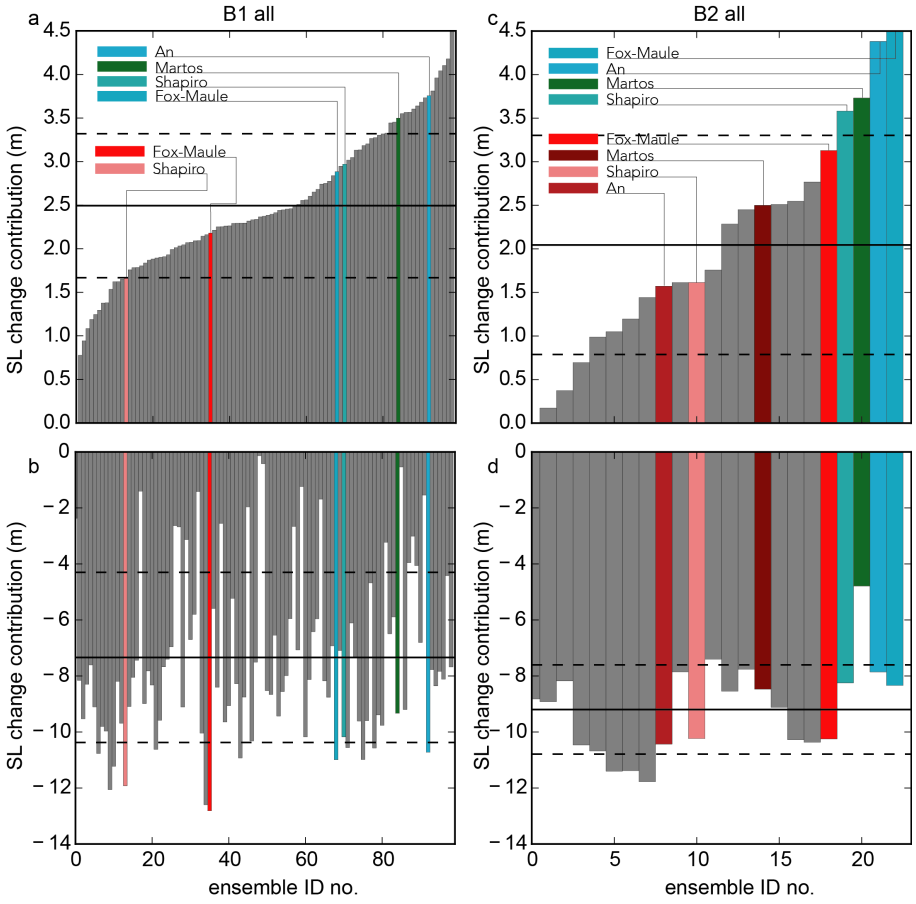

Figure 8. Sea level contribution in the LIG (a/c) and LGM (b/d) for the full ensemble forced with climate index~~glacial index~~ B1 and B2. The ensemble members focused on in this paper are highlighted by colours (P1 red colors, P2 blue/green colors). Horizontal black lines depict the full ensemble means and the dashed lines the standard deviations. The x-axis shows the individual ensemble IDs in ascending order of LIG SL contribution.

a strong influence on grounding line advance. A calving thickness of 75 m generally leads to a good representation of LGM ice margin reconstructions (Bentley et al., 2014) (Figure 7 b), while simulations with a thickness limit of 150 m underestimate Ross Sea LGM grounding line advance. Furthermore, the parameterisation of ice shelf calving can play a preeminent role in interglacials, which underlines the dire need for a physical rather than heuristic representation of calving in ice-sheet models.

The different forcing approaches of our study and Pollard and DeConto (2009); de Boer et al. (2014) and Tigchelaar et al. (2018) are apparent e.g. in the largest ice-sheet~~ice sheet~~ retreat ocurring in our ensemble at MIS5e while occurring during MIS 7 (ca. 210 kyr BP) for both Pollard and DeConto (2009) and de Boer et al. (2014) while in Tigchelaar et al. (2018) Quaternary ice-sheet~~ice sheet~~ volume never drops below the present AIS volume. ~~Note also, that the stability of the marine WAIS is crucially dependent on the choice of the GHF, as all simulations with the GHF field from Purucker (2013) exhibit a~~

collapse of the WAIS in the LIG with a much smaller loss for both Martos et al. (2017) and Shapiro and Ritzwoller (2004). In our simulations, the applied sea level forcing plays a minor role in the stability of the WAIS in lnterglacials (not shown).

3.2 The role of geothermal heat flux

It is a well established fact, that the heat flux at the ice-bedrock interface can be a major driver of ice-sheetice sheet evolutiondynamics. Albeit, the GHF for the AISAntaretic Ice Sheet is poorly constrained (Martos et al., 2017) and the few published continental data sets available differ substantially (see Figure 4 and Martos et al. (2017)). We can analyse the impact of GHF in our model ensemble by gauging the fit of diagnostic variables (ice thickness, basal melt, basal temperature, ice volume) in comparison to observed data. Both data sets from Purucker (2013) and An et al. (2015) show relatively low heat flux along the East Antarctic ice divide and overall for the WAIS. In consequence, potential "Oldest Ice" candidate sites indicated by the model ensemble and using those two data sets are unrealistically large, due to the absence of basal melting (see Figure 11), specifically for the Dome Fuji region. This is the case regardless of the model parameterisation and climate forcing or sea level input data. The choice of geothermal heat flux imprints on both East and West Antarctic ice thicknessdynamics., While mostly Modulating ice thickness (leading to thickness changes of up to 20%) in East Antarctica itbut also impactsimpacting the simulated ice divide along the transect of Dome A-Ridge B-Vostok-Dome C (see Figure 11). The impact of heat flux in West Antarctica can be drastic, as it acts as a major control on the marine ice-sheetice sheet instability. All simulations with the GHF field from Purucker (2013) exhibit a collapse of the WAIS in the LIG with a much smaller percentage for both Martos et al. (2017) and Shapiro and Ritzwoller (2004). A thorough analysis of this result is beyond the scope of this manuscript, but it could be caused by larger glacial ice cover caused by the colder basal conditions in Purucker (2013). This would lead to an overdeepened bedrock and larger surface gradients along the coast at the onset of interglacials and therefore to favourable conditions for the marine ice sheet instability. Overall ice-sheetice sheet variability between ensemble members (for identical parameter settings) due to different choices of GHF is consistently larger than due to the choice of different sea level forcing. This emphasises the strong role of GHF in modulating Antarctic Ice Sheet dynamics and overall evolution of ice volume.

3.3 Ice thickness variability in WAIS and EAIS

Ice thickness is an important parameter controlling the availability of a continuous 1.5 million year old ice core record at a given location. If the ice is too thick, its insulating properties lead to melting at the ice bedrock interface, if it is too thin, either old ice is transported away too quickly or the layering might be too thin to decipher a meaningful transient climate signal. Figures 9 and 10 show the ice thickness change at the four East and West Antarctic ice core locations which are depicted in Figure 1.

In the simulations with a collapsed late Pliocene WAIS (ensemble B2), the MPT leads to the advance of the WAIS into a present day configuration going along with a closure of the open ocean connection between the Weddell-, Amundsen/Bellinghausen- and Ross-Seas. However, in those simulations with no early Pleistocene WAIS, the WAIS remains relatively small throughout the Quaternary which is likely to be an indication that the climate forcing is too warm. The ensemble members with a stable

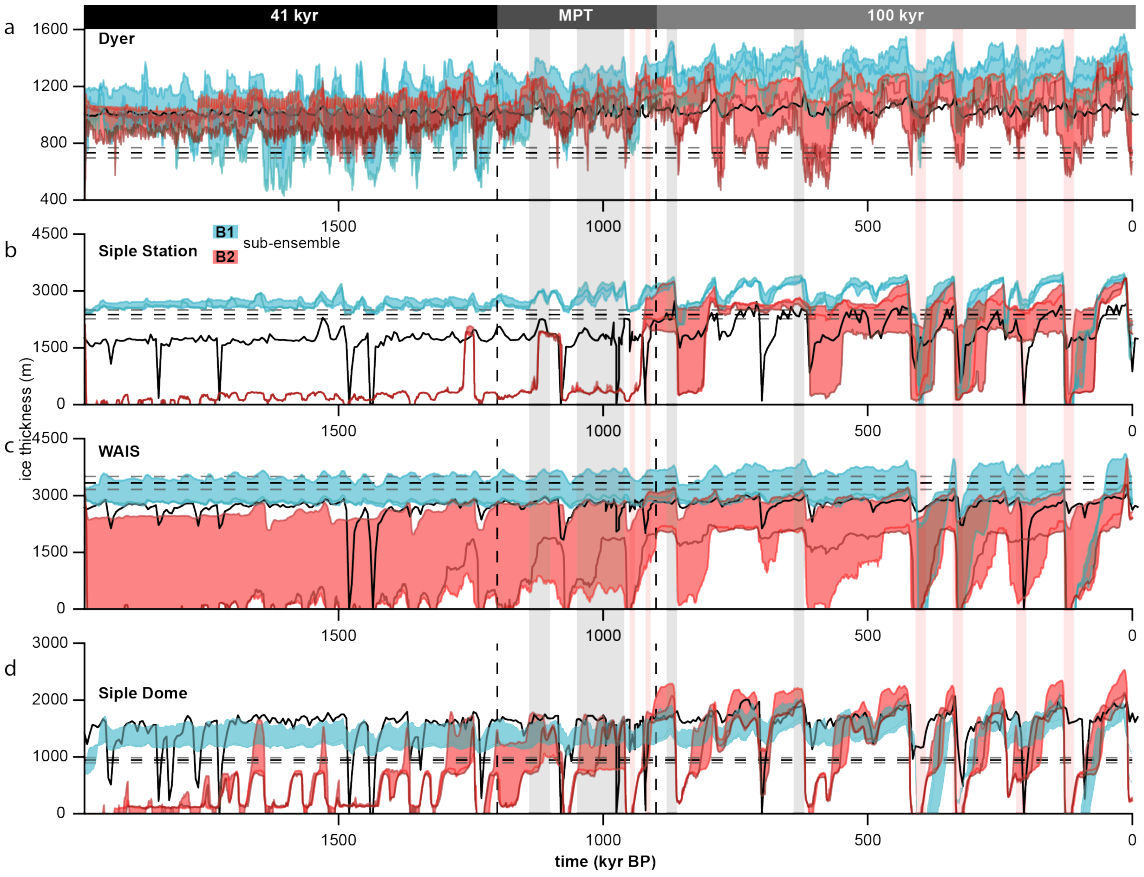

Figure 9. Ice thickness evolution during the last two Myr as simulated in our model ensemble for the four West Antarctic ice core locations (see Figure 1). Blue lines are from ensemble B1 (as in Figure 6) red lines from B2. Sampling rate is 1 kyr. For comparison, the ice thickness evolution simulated in Pollard and DeConto (2009) is plotted in black (sampling rate 10 kyr). The observed present day ice thickness, derived from BEDMAP2 (Fretwell et al., 2013), is shown by the horizontal black dashed line, with 5% variation illustrated by grey dashed lines. The ice thickness simulated in Pollard and DeConto (2009) is based on a 5 Myr transient simulation using BEDMAP1 (Lythe et al., 2001) as the initial ice-sheetice ~~sheet~~ configuration.

interglacial pre-MPT WAIS transition to a higher variability during the MPT with no major re-organisation of ice flow and grounding line dynamics.

Changes in the EAIS manifest in an increase in ice thickness ~~variability~~ across the MPT by ca. 30% (mean ice thickness at ice core locations calculated for pre-MPT (1.8-1.2 Myr BP) and Quaternary (0.8-0.0 Myr BP)) time intervals alongside an increase in variability in glacial-interglacial ice volume (standard deviation of ice thickness of individual ensemble members) of ca 50%. The shift to larger Glacial–Interglacial ice thickness changes in individual ensemble members is evident at all ice core locations and mostly due to the more pronounced climate cycles following the MPT. The temporal evolution of ice thickness

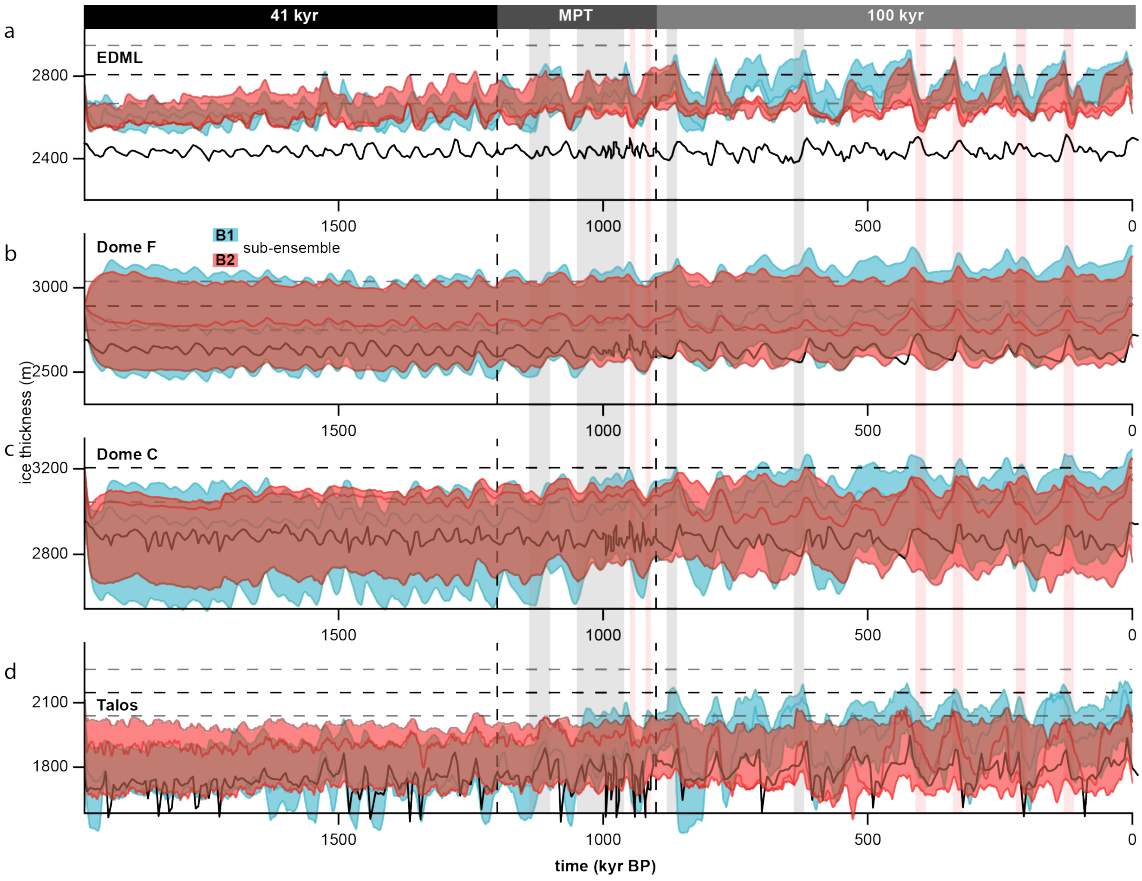

Figure 10. Same as Figure 9 but for the four East Antarctic ice cores.

changes for the different East Antarctic ice core locations follows a similar pattern with muted variability during the pre-MPT and a gradual increase completed by ca. 900 kyr BP. Note, that we find different points in time regarding ice thickness maxima for the central dome positions Dome C and Dome Fuji compared to positions away from the central Domes such as around the EDML and Talos Dome ice core sites. While the former generally show ice-sheetice sheet maxima during mid interglacials, the latter show maxima generally at the onset of interglacials and declining ice thicknesses during the interglacial. This and the higher glacial-interglacial variability for the two locations (EDML and Talos) can be explained by the impact of grounding line migration and larger glacial-interglacial surface mass balance differences. Mean ice thickness variability for Dome Fuji and Dome C during the late Quaternary is 165 and 195 m, respectively (105 and 140 during pre-MPT). Overall, the simulated present day ice thicknesscover after 2 Myr at the highlighted ice core locations in East Antarctica is in good agreement with the ice thickness derived from the BEDMAP2 (Fretwell et al., 2013) data set (within $\approx 5\%$ discrepancy in ice thickness for the selected ensemble members in B1 and B2). A notable exception is the Talos Dome ice thickness, which is too thin in all discussed B1 and B2 ensemble members except for the runs simulated with the relatively cold (Purucker, 2013) or

intermediate (Shapiro and Ritzwoller, 2004) GHF data set. The applied model resolution of 16 km is generally too coarse to accurately reconstruct smaller outlet glaciers and therefore might overestimate advection away from coastal ice domes.

3.4 Mapping potential Oldest Ice sites

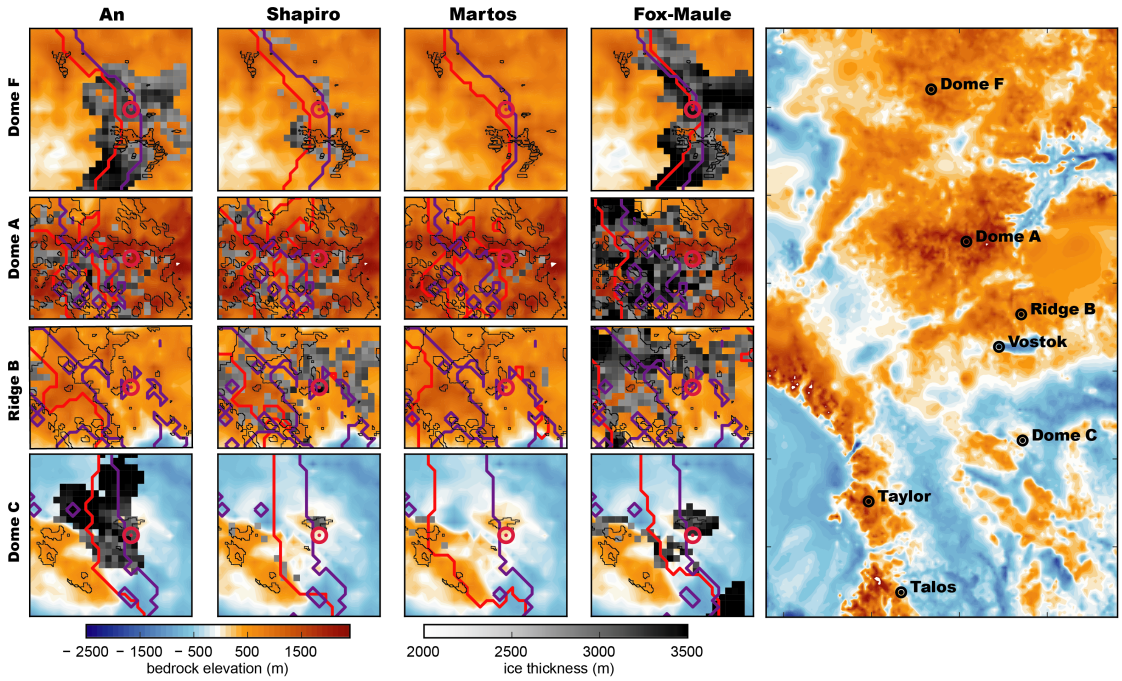

Figure 11. Comparison between regions of Oldest Ice identified in this study and in Van Liefferinge and Pattyn (2013) (Ridge B, Dome A) and Van Liefferinge et al. (2018) (Dome C, Dome Fuji) outlined by thick black lines. Regions of Oldest Ice are defined as grid nodes where ice thickness is larger than 2000 m, basal melting is zero and surface ice velocity slower than 1 m/a (respective boxes coloured in grayscale). The left four columns show magnified sections centred at Dome Fuji, Dome A, Ridge B and Dome C for identical parameter sets and forcing but different geothermal heat flux (from left An et al. (2015), Shapiro and Ritzwoller (2004), Martos et al. (2017) and Purucker (2013) GHF forcing). The red line in enlarged regions depicts the simulated present day ice divide (defined as position where surface elevation gradient switches direction), while the purple line depicts the present day ice divide as computed from BEDMAP2.

We apply the conditions for the existence of 1.5 Myr old ice derived in Fischer et al. (2013) (ice thickness larger than 2000 m, basal melting zero and surface ice velocity slower than 1 m/a) to our simulations in order to investigate the impact of the transient paleo-climate forcing, GHF and different model parameterisations on the sites Dome Fuji, Dome C, Dome A and Ridge B (Figure 11). Overall, we identify similar Oldest Ice regions as in Van Liefferinge and Pattyn (2013); Van Liefferinge et al. (2018); Parrenin et al. (2017); Passalacqua et al. (2017). This gives us confidence in the robustness of our model results and shows, that the transient forcing and continental setup used here does not change the general conclusions in Van Liefferinge et al. (2018). The regions with major overlaps to Van Liefferinge et al. (2018) are thus promising sites from a paleo ice-climate

evolution~~dynamics~~ viewpoint as well as from the detailed dissection of the present day conditions. Overall, applying the GHF from the data set by Shapiro and Ritzwoller (2004) yields the best agreement with the findings of Van Liefferinge and Pattyn (2013); Van Liefferinge et al. (2018); Parrenin et al. (2017) and Passalacqua et al. (2017). However, the geothermal heat flux data set from Martos et al. (2017) matches the observed/derived heat flux at Dome C to a better degree. In the simulations with the Martos et al. (2017) data set, the present day ice divide around Dome C is shifted strongly (ca. 160 km) in direction of the Ross Sea/Belgica Subglacial Highlands compared to the other three data sets due to the low geothermal heat flux south-west~~east~~ of the Dome C region contrasting with the high heat flux around Dome C (see Figure 11). Simulations using the Martos et al. (2017) data set show almost no viable conditions for the existence of Oldest Ice in East Antarctica (with the exception of oldest ice patches around Dome A, Ridge B and in the Belgica Subglacial Highlands west~~east~~ of Dome C), as basal temperatures are relatively high due to the large heat flux at the base of the ice leading to sustained basal melting. This is the case despite the relatively low ice thickness (and therefore insulation) simulated with the Martos et al. (2017) data set. Simulations with the Purucker (2013) and An et al. (2015) GHF reconstruction overestimate the Oldest Ice area substantially (showing viable conditions also for the Dome Fuji and Dome C ice core location where subglacial melting is observed). Interestingly however, the Purucker (2013) data sets yields the best agreement between the simulated and observed present day ice divide for Dome Fuji as well as Dome C. The effect of the geothermal heat flux forcing is not limited to the basal temperature of the ice, but also has a substantial impact on overall ice thickness (up to 20% change between forcing sets, see Figure 10, comparing the difference between simulations with different GHF in the same ensemble).

Our findings indicate, that the existence of Oldest Ice is not only dependent on the choice of GHF but can also be influenced by the applied climate forcing or ice flow parameterisation modulating the regions illustrated in Figure 11. Despite regional differences, all three sites (Dome Fuji, Dome C, Vostok/Ridge B) show suitable conditions for an Oldest Ice core throughout the last 1.5 Myr. This accounts for ensemble members using either the GHF from Shapiro and Ritzwoller (2004) or Purucker (2013) and An et al. (2015) (see Figure 11). However the later two show unreasonably large Oldest Ice patches. While previously identified regions of Oldest Ice (e.g. in the Dome C area (Parrenin et al., 2017)) are also identified in our model results, the regions of Oldest Ice at Dome Fuji are somewhat shifted in comparison to the findings in (Van Liefferinge and Pattyn, 2013) and (Van Liefferinge et al., 2018). This might be due to the different employed input data or ice dynamics simulated, or affected by differences in model resolution or the thermal state at the base of the ice. However, the generally robust agreement between high resolution studies (Van Liefferinge et al., 2018; Parrenin et al., 2017; Passalacqua et al., 2017) and our coarse resolution paleo dynamics approach strengthens the notion of viable conditions for Oldest Ice both at Dome Fuji and Dome C as well as Ridge B.

4 Conclusions

The search for the major drivers of the mid Pleistocene transition is ongoing, with ice sheets acting as a crucial component of climate system re-arrangement. Our model ensemble simulations indicate both rapid transitions and gradual growth of the

Antarctic Ice Sheet during the MPT, featuring the buildup of a large glacial ice mass in West Antarctica driven by extended glacial conditions and muted interglacials between 1.2 and 0.9 Myr BP. These findings fit well to the notion of a significant expansion~~expanse~~ of the Antarctic Ice Sheet around 0.9 Myr BP by Elderfield et al. (2012). However, we do not find a major re-organisation of the EAIS grounding line across the MPT which is in contrast to the theory that the EAIS transitioned from a mostly land based ice sheet to a marine configuration in this interval (Raymo et al., 2006). However, such a re-organisation cannot be excluded at this point, as several other modelling studies show potential phases of major EAIS grounding line retreat in the Pliocene or under strong interglacial conditions (DeConto and Pollard, 2016; Mengel and Levermann, 2014), and proxy reconstructions indicate large scale EAIS grounding line retreat in the late Pleistocene (Wilson et al., 2018). While we do not simulate a transition to a marine based EAIS in the Wilkes and Aurora Basins, such a process would certainly imprint on ice flow around LDC due to proximity alone. We do find a clear transition of the WAIS configuration around 0.9 Myr in model runs where warm boundary conditions led to a collapse of the WAIS in the late Pliocene but allowed for glaciation during the colder interglacials in the MPT. We argue that such a transition between an ice free ~~WAIS~~ and a present day WAIS-configuration around 900 kyr BP would have a potentially stronger influence on the global climate system (compared to an advance of the EAIS grounded ice margin) via the closing of the gateway between the Ross, Amundsen and Weddell Sea. Additionally, climate conditions favourable~~pertaining~~ for~~to~~ a retreated configuration of the EAIS ice margin (Raymo et al., 2006) would imply a collapsed WAIS according to ice-sheet~~ice sheet~~ modelling studies (Golledge et al., 2015; DeConto and Pollard, 2016; Sutter et al., 2016). Our study confirms a strong contribution of the Antarctic Ice Sheet to the LIG sea level highstand, with a mean contribution of 2.5-3 m (depending on the climate index~~glacial index~~ record used and the applied boundary conditions) and a maximum contribution of ca. 4.5 m, which is in line with previous studies by Golledge et al. (2015), Sutter et al. (2016) and DeConto and Pollard (2016). This corroborates the major impact of the Antarctic Ice Sheet on LIG global sea level (Dutton et al., 2015). The spatial pattern of GHF can be decisive in modelling dynamics of the WAIS. Despite this uncertainty, we identify promising candidate sites at Dome Fuji, Dome C and Ridge B which provide favourable conditions for the existence of old ice throughout the last 2 Myr. This study illustrates that uncertainties in climate forcing and boundary conditions have a large impact on paleoclimate ice-sheet~~ice sheet~~ simulations and therefore the assessment of Oldest Ice sites ~~on long time scales~~. Accordingly, the successful retrieval of an ice core spanning the last 1.5 Myr would provide a transient data benchmark and proxy horizons against which ice-sheet~~ice sheet~~ models can be calibrated.~~tuned and providing insights into a potential major re-arrangement of the East Antarctic coastal margin during the MPT.~~

Code and data availability. PISM is freely available via github, we use PISM v0.73 with modifications. Further details on the code modifications can be provided upon request. Diagnostic ice sheet model output data is available upon request.

Competing interests. O. Eisen is CEIC of The Cryosphere

Acknowledgements. We would like to thank Bas de Boer, Jorge Bernales and the editor Alexander Robinson for their very constructive comments in the review process. We thank the regional climate initiative REKLIM and the AWI Strategy Fund for funding of the project. We express our gratitude to Christian Stepanek, Madlene Pfeiffer and Martin Werner for providing climate snapshot data from the ESM COSMOS. We are very grateful to Adrien Michel for providing the temperature reconstruction for ensemble branch B1. Hubertus Fischer gratefully acknowledges the long-term support by the Swiss National Science Foundation (SNSF). This publication was generated in the frame of Beyond EPICA-Oldest Ice (BE-OI). The project has received funding from the European Union's Horizon 2020 research and innovation programme under grant agreement no. 730258 (BE-OI CSA). It has received funding from the Swiss State Secretariate for Education, Research and Innovation (SERI) under contract number 16.0144. It is furthermore supported by national partners and funding agencies in Belgium, Denmark, France, Germany, Italy, Norway, Sweden, Switzerland, the Netherlands, and the United Kingdom. Logistic support is mainly provided by AWI, BAS, ENEA, and IPEV. The opinions expressed and arguments employed herein do not necessarily reflect the official views of the European Union funding agency, the Swiss Government, or other national funding bodies. The work of T.K. has been conducted in the framework of the PalMod project (FKZ: 01LP1511B), supported by the German Federal Ministry of Education and Research (BMBF) as Research for Sustainability initiative (FONA).

Development of PISM is supported by NASA grant NNX17AG65G and NSF grants PLR-1603799 and PLR-1644277.

This is BE-OI publication number 7.

The article processing charges for this open-access publication were covered by a Research Centre of the Helmholtz Association.

References

Abe-Ouchi, A., Saito, F., Kawamura, K., Raymo, M. E., Okuno, J., Takahashi, K., and Blatter, H.: Insolation-driven 100,000-year glacial cycles and hysteresis of ice-sheet volume, Nature, 500, 190–194, https://doi.org/https://doi.org/10.1038/nature12374, 2013.

Albrecht, T. and Levermann, A.: Fracture-induced softening for large-scale ice dynamics, Cryosphere, 8, 587–605, https://doi.org/Doi 10.5194/Tc-8-587-2014, 2014.

An, M. J., Wiens, D. A., Zhao, Y., Feng, M., Nyblade, A., Kanao, M., Li, Y. S., Maggi, A., and Leveque, J. J.: Temperature, lithosphere-asthenosphere boundary, and heat flux beneath the Antarctic Plate inferred from seismic velocities, Journal of Geophysical Research-Solid Earth, 120, 8720–8742, https://doi.org/10.1002/2015jb011917, 2015.

Bazin, L., Landais, A., Lemieux-Dudon, B., Toyé Mahamadou Kele, H., Veres, D., Parrenin, F., Martinerie, P., Ritz, C., Capron, E., Lipenkov, V., Loutre, M.-F., Raynaud, D., Vinther, B., Svensson, A., Rasmussen, S. O., Severi, M., Blunier, T., Leuenberger, M., Fischer, H., Masson-Delmotte, V., Chappellaz, J., and Wolff, E.: An optimized multi-proxy, multi-site Antarctic ice and gas orbital chronology (AICC2012): 120ndash;800 ka, Climate of the Past, 9, 1715–1731, https://doi.org/10.5194/cp-9-1715-2013, https://www.clim-past.net/9/1715/2013/, 2013.

Beckmann, A. and Goosse, H.: A parameterization of ice shelf-ocean interaction for climate models, Ocean Modelling, 5, 157–170, https://doi.org/https://doi.org/10.1016/S1463-5003(02)00019-7, 2003.

Bentley, M. J., Cofaigh, C. O., Anderson, J. B., Conway, H., Davies, B., Graham, A. G. C., Hillenbrand, C. D., Hodgson, D. A., Jamieson, S. S. R., Larter, R. D., Mackintosh, A., Smith, J. A., Verleyen, E., Ackert, R. P., Bart, P. J., Berg, S., Brunstein, D., Canals, M., Colhoun, E. A., Crosta, X., Dickens, W. A., Domack, E., Dowdeswell, J. A., Dunbar, R., Ehrmann, W., Evans, J., Favier, V., Fink, D., Fogwill, C. J., Glasser, N. F., Gohl, K., Golledge, N. R., Goodwin, I., Gore, D. B., Greenwood, S. L., Hall, B. L., Hall, K., Hedding, D. W., Hein, A. S., Hocking, E. P., Jakobsson, M., Johnson, J. S., Jomelli, V., Jones, R. S., Klages, J. P., Kristoffersen, Y., Kuhn, G., Leventer, A., Licht, K., Lilly, K., Lindow, J., Livingstone, S. J., Masse, G., McGlone, M. S., McKay, R. M., Melles, M., Miura, H., Mulvaney, R., Nel, W., Nitsche, F. O., O'Brien, P. E., Post, A. L., Roberts, S. J., Saunders, K. M., Selkirk, P. M., Simms, A. R., Spiegel, C., Stolldorf, T. D., Sugden, D. E., van der Putten, N., van Ommen, T., Verfaillie, D., Vyverman, W., Wagner, B., White, D. A., Witus, A. E., Zwartz, D., and Consortium, R.: A community-based geological reconstruction of Antarctic Ice Sheet deglaciation since the Last Glacial Maximum, Quaternary Science Reviews, 100, 1–9, https://doi.org/10.1016/j.quascirev.2014.06.025, 2014.

Bintanja, R. and van de Wal, R. S. W.: North American ice-sheet dynamics and the onset of 100,000-year glacial cycles, Nature, 454, 869–872, https://doi.org/https://doi.org/10.1038/nature07158, 2008.

Bueler, E. and Brown, J.: Shallow shelf approximation as a "sliding law" in a thermomechanically coupled ice sheet model, Journal of Geophysical Research-Earth Surface, 114, https://doi.org/https://doi.org/10.1029/2008JF001179, 2009.

Cavitte, M. G. P., Parrenin, F., Ritz, C., Young, D. A., Van Liefferinge, B., Blankenship, D. D., Frezzotti, M., and Roberts, J. L.: Accumulation patterns around Dome C, East Antarctica, in the last 73 kyr, Cryosphere, 12, 1401–1414, https://doi.org/10.5194/tc-12-1401-2018, 2018.

Chalk, T. B., Hain, M. P., Foster, G. L., Rohling, E. J., Sexton, P. F., Badger, M. P. S., Cherry, S. G., Hasenfratz, A. P., Haug, G. H., Jaccard, S. L., Martinez-Garcia, A., Palike, H., Pancost, R. D., and Wilson, P. A.: Causes of ice age intensification across the Mid-Pleistocene Transition, Proceedings of the National Academy of Sciences of the United States of America, 114, 13 114–13 119, https://doi.org/10.1073/pnas.1702143114, 2017.

Clark, P. U. and Pollard, D.: Origin of the middle Pleistocene transition by ice sheet erosion of regolith, Paleoceanography, 13, 1–9, https://doi.org/Doi 10.1029/97pa02660, 1998.

de Boer, B., Lourens, L. J., and van de Wal, R. S. W.: Persistent 400,000-year variability of Antarctic ice volume and the carbon cycle is revealed throughout the Plio-Pleistocene, Nature Communications, 5, https://doi.org/https://doi.org/10.1038/ncomms3999, 2014.

DeConto, R. M. and Pollard, D.: Contribution of Antarctica to past and future sea-level rise, Nature, 531, 591–597, https://doi.org/10.1038/nature17145, 2016.

Depoorter, M. A., Bamber, J. L., Griggs, J. A., Lenaerts, J. T. M., Ligtenberg, S. R. M., van den Broeke, M. R., and Moholdt, G.: Calving fluxes and basal melt rates of Antarctic ice shelves, Nature, 502, 89–93, https://doi.org/https://doi.org/10.1038/nature12567, 2013.

Dutton, A., Carlson, A. E., Long, A. J., Milne, G. A., Clark, P. U., DeConto, R., Horton, B. P., Rahmstorf, S., and Raymo, M. E.: Sea-level rise due to polar ice-sheet mass loss during past warm periods, Science, 349, https://doi.org/ARTN aaa4019 10.1126/science.aaa4019, 2015.

Elderfield, H., Ferretti, P., Greaves, M., Crowhurst, S., McCave, I. N., Hodell, D., and Piotrowski, A. M.: Evolution of Ocean Temperature and Ice Volume Through the Mid-Pleistocene Climate Transition, Science, 337, 704–709, https://doi.org/10.1126/science.1221294, 2012.

Feldmann, J., Albrecht, T., Khroulev, C., Pattyn, F., and Levermann, A.: Resolution-dependent performance of grounding line motion in a shallow model compared with a full-Stokes model according to the MISMIP3d intercomparison, Journal of Glaciology, 60, 353–360, https://doi.org/10.3189/2014JoG13J093, 2014.

Fischer, H., Severinghaus, J., Brook, E., Wolff, E., Albert, M., Alemany, O., Arthern, R., Bentley, C., Blankenship, D., Chappellaz, J., Creyts, T., Dahl-Jensen, D., Dinn, M., Frezzotti, M., Fujita, S., Gallee, H., Hindmarsh, R., Hudspeth, D., Jugie, G., Kawamura, K., Lipenkov, V., Miller, H., Mulvaney, R., Parrenin, F., Pattyn, F., Ritz, C., Schwander, J., Steinhage, D., van Ommen, T., and Wilhelms, F.: Where to find 1.5 million yr old ice for the IPICS "Oldest-Ice" ice core, Climate of the Past, 9, 2489–2505, https://doi.org/Doi 10.5194/Cp-9-2489-2013, 2013.

Fretwell, P., Pritchard, H. D., Vaughan, D. G., Bamber, J. L., Barrand, N. E., Bell, R., Bianchi, C., Bingham, R. G., Blankenship, D. D., Casassa, G., Catania, G., Callens, D., Conway, H., Cook, A. J., Corr, H. F. J., Damaske, D., Damm, V., Ferraccioli, F., Forsberg, R., Fujita, S., Gim, Y., Gogineni, P., Griggs, J. A., Hindmarsh, R. C. A., Holmlund, P., Holt, J. W., Jacobel, R. W., Jenkins, A., Jokat, W., Jordan, T., King, E. C., Kohler, J., Krabill, W., Riger-Kusk, M., Langley, K. A., Leitchenkov, G., Leuschen, C., Luyendyk, B. P., Matsuoka, K., Mouginot, J., Nitsche, F. O., Nogi, Y., Nost, O. A., Popov, S. V., Rignot, E., Rippin, D. M., Rivera, A., Roberts, J., Ross, N., Siegert, M. J., Smith, A. M., Steinhage, D., Studinger, M., Sun, B., Tinto, B. K., Welch, B. C., Wilson, D., Young, D. A., Xiangbin, C., and Zirizzotti, A.: Bedmap2: improved ice bed, surface and thickness datasets for Antarctica, Cryosphere, 7, 375–393, https://doi.org/Doi 10.5194/Tc-7-375-2013, 2013.

Frieler, K., Clark, P. U., He, F., Buizert, C., Reese, R., Ligtenberg, S. R. M., van den Broeke, M. R., Winkelmann, R., and Levermann, A.: Consistent evidence of increasing Antarctic accumulation with warming, Nature Climate Change, 5, 348–352, 2015.

Ganopolski, A. and Brovkin, V.: Simulation of climate, ice sheets and CO_2 evolution during the last four glacial cycles with an Earth system model of intermediate complexity, Climate of the Past, 13, 1695–1716, https://doi.org/10.5194/cp-13-1695-2017, 2017.

Gladstone, R. M., Payne, A. J., and Cornford, S. L.: Parameterising the grounding line in flow-line ice sheet models, Cryosphere, 4, 605–619, https://doi.org/Doi 10.5194/Tc-4-605-2010, 2010.

Golledge, N. R., Menviel, L., Carter, L., Fogwill, C. J., England, M. H., Cortese, G., and Levy, R. H.: Antarctic contribution to meltwater pulse 1A from reduced Southern Ocean overturning, Nature Communications, 5, https://doi.org/ARTN 5107 10.1038/ncomms6107, 2014.

Golledge, N. R., Kowalewski, D. E., Naish, T. R., Levy, R. H., Fogwill, C. J., and Gasson, E. G. W.: The multi-millennial Antarctic commitment to future sea-level rise, Nature, 526, 421–+, https://doi.org/10.1038/nature15706, 2015.

Jouzel, J., Masson-Delmotte, V., Cattani, O., Dreyfus, G., Falourd, S., Hoffmann, G., Minster, B., Nouet, J., Barnola, J. M., Chappellaz, J., Fischer, H., Gallet, J. C., Johnsen, S., Leuenberger, M., Loulergue, L., Luethi, D., Oerter, H., Parrenin, F., Raisbeck, G., Raynaud, D., Schilt, A., Schwander, J., Selmo, E., Souchez, R., Spahni, R., Stauffer, B., Steffensen, J. P., Stenni, B., Stocker, T. F., Tison, J. L., Werner, M., and Wolff, E. W.: Orbital and millennial Antarctic climate variability over the past 800,000 years, Science, 317, 793–796, https://doi.org/Doi 10.1126/Science.1141038, 2007.

Karlsson, N. B., Binder, T., Eagles, G., Helm, V., Pattyn, F., Van Liefferinge, B., and Eisen, O.: Glaciological characteristics in the Dome Fuji region and new assessment for "Oldest Ice", Cryosphere, 12, 2413–2424, https://doi.org/10.5194/tc-12-2413-2018, 2018.

Konrad, H., Thoma, M., Sasgen, I., Klemann, V., Grosfeld, K., Barbi, D., and Martinec, Z.: The Deformational Response of a Viscoelastic Solid Earth Model Coupled to a Thermomechanical Ice Sheet Model, Surveys in Geophysics, 35, 1441–1458, https://doi.org/Doi 10.1007/S10712-013-9257-8, 2014.

Larour, E., Morlighem, M., Seroussi, H., Schiermeier, J., and Rignot, E.: Ice flow sensitivity to geothermal heat flux of Pine Island Glacier, Antarctica, Journal of Geophysical Research-Earth Surface, 117, https://doi.org/https://doi.org/10.1029/2012JF002371, 2012.

Lazeroms, W. M. J., Jenkins, A., Gudmundsson, G. H., and van de Wal, R. S. W.: Modelling present-day basal melt rates for Antarctic ice shelves using a parametrization of buoyant meltwater plumes, Cryosphere, 12, 49–70, https://doi.org/10.5194/tc-12-49-2018, 2018.

Lisiecki, L. E. and Raymo, M. E.: A Pliocene-Pleistocene stack of 57 globally distributed benthic delta O-18 records, Paleoceanography, 20, https://doi.org/https://doi.org/10.1029/2004PA001071, 2005.

Locarnini, R. A., Mishonov, A. V., Antonov, J. I., Boyer, T. P., Garcia, H. E., Baranova, O. K., Zweng, M. M., and Johnson, D. R.: World Ocean Atlas 2009, Volume 1: Temperature., NOAA Atlas NESDIS 68, U.S. Government Printing Office, 2010.

Lunt, D. J., Abe-Ouchi, A., Bakker, P., Berger, A., Braconnot, P., Charbit, S., Fischer, N., Herold, N., Jungclaus, J. H., Khon, V. C., Krebs-Kanzow, U., Langebroek, P. M., Lohmann, G., Nisancioglu, K. H., Otto-Bliesner, B. L., Park, W., Pfeiffer, M., Phipps, S. J., Prange, M., Rachmayani, R., Renssen, H., Rosenbloom, N., Schneider, B., Stone, E. J., Takahashi, K., Wei, W., Yin, Q., and Zhang, Z. S.: A multi-model assessment of last interglacial temperatures, Climate of the Past, 9, 699–717, 2013.

Lythe, M. B., Vaughan, D. G., and Consortium, B.: BEDMAP: A new ice thickness and subglacial topographic model of Antarctica, Journal of Geophysical Research-Solid Earth, 106, 11 335–11 351, https://doi.org/Doi 10.1029/2000jb900449, 2001.

Martos, Y. M., Catalan, M., Jordan, T. A., Golynsky, A., Golynsky, D., Eagles, G., and Vaughan, D. G.: Heat Flux Distribution of Antarctica Unveiled, Geophysical Research Letters, 44, 11 417–11 426, https://doi.org/10.1002/2017gl075609, 2017.

Mengel, M. and Levermann, A.: Ice plug prevents irreversible discharge from East Antarctica, Nature Climate Change, 4, 451–455, https://doi.org/Doi 10.1038/Nclimate2226, 2014.

Michel, A., Schwander, J., and Fischer, H.: Transient Modeling of Borehole Temperature and Basal Melting in an Ice Sheet, Master Thesis, Climate and Environmental Physics Institute, University of Bern, 2016.

Parrenin, F., Cavitte, M. G. P., Blankenship, D. D., Chappellaz, J., Fischer, H., Gagliardini, O., Masson-Delmotte, V., Passalacqua, O., Ritz, C., Roberts, J., Siegert, M. J., and Young, D. A.: Is there 1.5-million-year-old ice near Dome C, Antarctica?, Cryosphere, 11, 2427–2437, https://doi.org/10.5194/tc-11-2427-2017, 2017.

Passalacqua, O., Ritz, C., Parrenin, F., Urbini, S., and Frezzotti, M.: Geothermal flux and basal melt rate in the Dome C region inferred from radar reflectivity and heat modelling, Cryosphere, 11, 2231–2246, https://doi.org/10.5194/tc-11-2231-2017, 2017.

Pfeiffer, M. and Lohmann, G.: Greenland Ice Sheet influence on Last Interglacial climate: global sensitivity studies performed with an atmosphere-ocean general circulation model, Climate of the Past, 12, 1313–1338, https://doi.org/10.5194/cp-12-1313-2016, 2016.

Pollard, D. and DeConto, R. M.: Modelling West Antarctic ice sheet growth and collapse through the past five million years, Nature, 458, 329–333, 2009.

Pollard, D. and DeConto, R. M.: Description of a hybrid ice sheet-shelf model, and application to Antarctica, Geoscientific Model Development, 5, 1273–1295, https://doi.org/10.5194/gmd-5-1273-2012, 2012.

Purucker, M. E.: Geothermal heat flux data set based on low res- olution observations collected by the CHAMP satellite be- tween 2000 and 2010, and produced from the MF-6 model following the technique described in Fox Maule et al. (2005), retrieved from: https:core2.gsfc.nasa.govresearchpuruckerheatflux_updates.html, 2013.

Raymo, M. E. and Huybers, P.: Unlocking the mysteries of the ice ages, Nature, 451, 284–285, https://doi.org/10.1038/nature06589, 2008.

Raymo, M. E., Lisiecki, L. E., and Nisancioglu, K. H.: Plio-pleistocene ice volume, Antarctic climate, and the global delta O-18 record, Science, 313, 492–495, https://doi.org/10.1126/science.1123296, 2006.

Reese, R., Gudmundsson, G. H., Levermann, A., and Winkelmann, R.: The far reach of ice-shelf thinning in Antarctica, Nature Climate Change, 8, 53–+, https://doi.org/10.1038/s41558-017-0020-x, 2018.

Rignot, E., Jacobs, S., Mouginot, J., and Scheuchl, B.: Ice-Shelf Melting Around Antarctica, Science, 341, 266–270, https://doi.org/10.1126/science.1235798, 2013.

Rohling, E. J., Foster, G. L., Grant, K. M., Marino, G., Roberts, A. P., Tamisiea, M. E., and Williams, F.: Sea-level and deep-sea-temperature variability over the past 5.3 million years (vol 508, pg 477, 2014), Nature, 510, 432–432, https://doi.org/10.1038/nature13488, 2014.

Schoof, C.: Coulomb Friction and Other Sliding Laws in a Higher-Order Glacier Flow Model, Mathematical Models & Methods in Applied Sciences, 20, 157–189, https://doi.org/10.1142/S0218202510004180, 2010.

Shapiro, N. M. and Ritzwoller, M. H.: Inferring surface heat flux distributions guided by a global seismic model: particular application to Antarctica, Earth and Planetary Science Letters, 223, 213–224, https://doi.org/Doi 10.1016/J.Epsl.2004.04.011, 2004.

Snyder, C. W.: Evolution of global temperature over the past two million years, Nature, 538, 226–228, https://doi.org/10.1038/nature19798, 2016.

Stepanek, C. and Lohmann, G.: Modelling mid-Pliocene climate with COSMOS, Geoscientific Model Development, 5, 1221–1243, https://doi.org/10.5194/gmd-5-1221-2012, 2012.

Sutter, J., Gierz, P., Grosfeld, K., Thoma, M., and Lohmann, G.: Ocean temperature thresholds for Last Interglacial West Antarctic Ice Sheet collapse, Geophysical Research Letters, 43, 2675–2682, https://doi.org/10.1002/2016gl067818, 2016.

Tigchelaar, M., Timmermann, A., Pollard, D., Friedrich, T., and Heinemann, M.: Local insolation changes enhance Antarctic interglacials: Insights from an 800,000-year ice sheet simulation with transient climate forcing, Earth and Planetary Science Letters, 495, 69–78, https://doi.org/10.1016/j.epsl.2018.05.004, 2018.

Van Liefferinge, B. and Pattyn, F.: Using ice-flow models to evaluate potential sites of million year-old ice in Antarctica, Climate of the Past, 9, 2335–2345, https://doi.org/Doi 10.5194/Cp-9-2335-2013, 2013.

Van Liefferinge, B., Pattyn, F., Cavitte, M. G. P., Karlsson, N. B., Young, D. A., Sutter, J., and Eisen, O.: Promising Oldest Ice sites in East Antarctica based on thermodynamical modelling, Cryosphere, 12, 2773–2787, https://doi.org/10.5194/tc-12-2773-2018, 2018.

van Wessem, J. M., Reijmer, C. H., Morlighem, M., Mouginot, J., Rignot, E., Medley, B., Joughin, I., Wouters, B., Depoorter, M. A., Bamber, J. L., Lenaerts, J. T. M., van de Berg, W. J., van den Broeke, M. R., and van Meijgaard, E.: Improved representation of East Antarctic surface mass balance in a regional atmospheric climate model, Journal of Glaciology, 60, 761–770, https://doi.org/10.3189/2014JoG14J051, 2014.

Veres, D., Bazin, L., Landais, A., Toyé Mahamadou Kele, H., Lemieux-Dudon, B., Parrenin, F., Martinerie, P., Blayo, E., Blunier, T., Capron, E., Chappellaz, J., Rasmussen, S. O., Severi, M., Svensson, A., Vinther, B., and Wolff, E. W.: The Antarctic ice core chronology (AICC2012): an optimized multi-parameter and multi-site dating approach for the last 120 thousand years, Climate of the Past, 9, 1733–1748, https://doi.org/10.5194/cp-9-1733-2013, https://www.clim-past.net/9/1733/2013/, 2013.

Werner, M., Jouzel, J., Masson-Delmotte, V., and Lohmann, G.: Reconciling glacial Antarctic water stable isotopes with ice sheet topography and the isotopic paleothermometer, Nature Communications, 9, https://doi.org/ARTN 3537 10.1038/s41467-018-05430-y, 2018.

Wilson, D. J., Bertram, R. A., Needham, E. F., van de Flierdt, T., Welsh, K. J., McKay, R. M., Mazumder, A., Riesselman, C. R., Jimenez-Espejo, F. J., and Escutia, C.: Ice loss from the East Antarctic Ice Sheet during late Pleistocene interglacials, Nature, 561, 383–386, https://doi.org/10.1038/s41586-018-0501-8, 2018.

Winkelmann, R., Martin, M. A., Haseloff, M., Albrecht, T., Bueler, E., Khroulev, C., and Levermann, A.: The Potsdam Parallel Ice Sheet Model (PISM-PIK) - Part 1: Model description, Cryosphere, 5, 715–726, https://doi.org/Doi 10.5194/Tc-5-715-2011, 2011.

Young, D. A., Roberts, J. L., Ritz, C., Frezzotti, M., Quartini, E., Cavitte, M. G. P., Tozer, C. R., Steinhage, D., Urbini, S., Corr, H. F. J., van Ommen, T., and Blankenship, D. D.: High-resolution boundary conditions of an old ice target near Dome C, Antarctica, Cryosphere, 11, 1897–1911, https://doi.org/10.5194/tc-11-1897-2017, 2017.

Yu, H., Rignot, E., Seroussi, H., and Morlighem, M.: Retreat of Thwaites Glacier, West Antarctica, over the next 100 years using various ice flow models, ice shelf melt scenarios and basal friction laws, The Cryosphere, 12, 3861–3876, https://doi.org/10.5194/tc-12-3861-2018, 2018.

We thank Jorge Alvarez-Solas for his thorough review on our paper and for his constructive comments and remarks. We hope that we are able to address them in a satisfactory manner and discuss the modifications we introduced motivated by his remarks below. Please find all changes and the new or modified figures in the attached manuscript tracked in red. We also included the main changes below each comment in this document in red and our response to the reviewer's comments in blue.

1) Main goal of the study:

I think this study nicely focuses on providing new information on where to look for the oldest Antarctic ice within the framework of continentally wide ice-sheet modeling. And it is also appreciable to subscribe such an approach within the context of transient simulations covering the MPT.

Nevertheless, several parts of the abstract and the introduction can be misleading because they are somehow suggesting that an important part of the paper will be devoted to analyze the effects of parametric uncertainty on the Antarctic ice dynamics during the MPT.

For example, the abstract reads: "We discuss the effects of changing climate conditions, sea level and geothermal heat flux boundary conditions on the mass balance and ice dynamics of the Antarctic Ice Sheet." This is not strictly true, particularly so with respect to ice dynamics (there is not a single panel or comment devoted to ice velocities or changes in the ice flow dynamics as a result of the changing climate). Changes in the grounding line position (also very superficially tackled), basal temperature and thickness evolution are related to changes in ice velocities, but this relationship is not addressed in the paper.

Similar misleading sentences to that of the abstract mentioned above can be found throughout the introduction (e.g. page 2, lines 27-29) and methods (page 7, lines 5-7).

I suggest two different ways of mitigating this issue:

a) Lower the reader's expectations concerning ice dynamics.
b) Expand the analysis on the effects that different parameters controlling the ice flow have on the conclusions of the study.

We concur with the reviewer, that the use of the term "dynamics" can potentially misguide the reader's expectations. While we do discuss e.g. grounding line migration in the Last Interglacial we do not dive into the intricacies of e.g. ice flow changes and individual rerouting of outlet glaciers. We rather put the focus on ice thickness changes around Oldest Ice candidate sites and analyse ice volume throughout the last 2 million years as an integrative measure of configurational changes of the Antarctic Ice Sheet. We appreciate the reviewer's suggestion to rephrase certain parts of the manuscript to lower the readers expectations with regard to the term "dynamics". While rewriting the manuscript with a detailed focus on ice dynamical changes during the last 2 Million years would be certainly worthwhile, we think that this would be better suited for a separate manuscript and would divert too much attention from the main focus of this study: to identify potential Oldest Ice sites for the IPICS endeavour.

We rephrased all potentially misleading sentences containing the term "dynamics" in the manuscript.

2) Reproducibility and description of the methods:

The manuscript contains a large amount of small inaccuracies, typos and erratum, particularly so in the methods section. These, taken individually, do not constitute a major problem, but taken together have a double negative effect: i) do not allow for the suitable reproducibility of this study, and ii) make the reading of the manuscript frustrating.

SPECIFIC COMMENTS

1) Ice-sheet model and ensembles

Page 4, line 29 reads: "[...] we linearly scale the computed present day melt rates in the Amundsen and Bellinghausen Sea by a factor of 10 and underneath the Filchner Ice Shelf by a factor of 1.5. Shelf melt rates adjacent to Wilkes, Terre Adelie and George V Land in East Antarctica are also scaled by factor of 10."
What do these scaling factors do?
Are they simply multiplying (or dividing) the observed values? Please define.

This is indeed not self explanatory, we therefore add a short sentence clarifying, that the scaling factors multiply the computed melt rates.

P5, l8 -

To better match present day observed sub ice-shelf melt rates (Rignot et al., 2013; Depoorter et al., 2013), we had to multiply the computed present day melt rates in the Amundsen and Bellinghausen Sea by a factor of m_b=10, around the Antarctic Peninsula by 5, and underneath the Filchner Ice Shelf by a factor of 1.5. Shelf melt rates adjacent to Wilkes, Terre Adelie and George V Land in East Antarctica are also scaled by factor of 10 in a subset of the simulations.

Furthermore, the above quoted sentence seems incongruent with having a parameter between 1 and 10 as a part of the ensemble controlling the basal melt values (gamma_EAIS [1;10]).
Caption of table 2 refers to George V and Wilkes Lands, while the above scaling factors refer to other basins as well.
Thus, are the values of the shelf melt being changed as a part of the ensemble? If yes,
both basins simultaneously?
On the other hand, if these scaling factors reflect the uncertainty associated to the processes that determine shelf basal melt in time, why not exploring the factors of the rest of the basins as well?
Please define and clarify.

We agree with the reviewer that this is unclear in the manuscript. Table 2 is now revised according to the suggestions of both reviewers and provides the two main parameter sets discussed in the manuscript, while additionally providing further parameter combinations used in the ensemble but not discussed in the results. We now address specifically which ensemble members are mainly analysed in

the study (p10, l4-11) and changed table 2 (p10) accordingly. Table 2 now provides the two main parameter sets used for all sea level and geothermal heat flux combinations in ensemble B1 and for all geothermal heat flux combinations in B2. We further provide additional parameter combinations simulated in the ensemble but not discussed in the manuscript in the third line of table 2. We hope this clarifies the main scope of the ensemble.

P10, l4-11

The constituting forcing set for the ensemble consists of four different geothermal heat flux and three sea level data sets, i.e. twelve individual experimental settings. We further explore two main parameter sets (P1 and P2) highlighted in table 2. While we do take into account all sea level variations for ensemble B1 (48 individual experiments), we only look at the sea level forcing derived from Lisiecki and Raymo (2005) (LR05) in ensemble B2. We also experimented with other parameter choices based on table 2 (VP) but not covering all individual forcing sets, thus these are not discussed in this study. The ensemble members discussed in this manuscript consist of 8 experiments for each ensemble B1 and B2 with sea level forcing from LR05.

Table 2. Selected ISM parameters for the model ensemble. First and second line show the main parameter sets used in the ensemble (P1 and P2). The third line lists additional parameters tested but not further explored (VP). cH stands for thickness calving limit (in meter), cE is a parameter in the Eigencalving equation. sia_e and ssa_e stand for the so called sia and ssa "enhancement factors", $till_{min}$ and $till_{max}$ modify basal friction in the sliding law. γ_{EAIS} is a dimensionless scaling factor for basal shelf melt for selected East Antarctic ice shelf regions (George V Land, Wilkes Land).

Parameter	sia_e	ssa_e	cH (m)	cE	$till_{min}$	$till_{max}$	γ_{EAIS}
P1	1.0	0.55	**75**	$1 \cdot 10^{17}$	5	30	**10**
P2	1.0	0.55	**150**	$1 \cdot 10^{17}$	5	30	**1**
VP	1.6 ; 1.7 ; 2.0	1.0	100	$1 \cdot 10^{18}$	10	40	5-20

How is the shelf basal melting evolution in time achieved in the model? Is it dependent on the temperatures of the ocean given by equation 2?
If yes, how is it done? Perhaps an anomaly method with respect to the scaled PD basal melt defined in page 4, line 29?
Please define.

Basal melt rates are calculated according to the formulation in Beckmann and Goosse (2003) with a square dependency on the temperature difference between the pressure dependent freezing point and the ambient ocean temperature as used in e.g. Pollard and DeConto (2012). We added the melt rate equation on p5. The ocean temperature over time is derived as shown in equation 4.

$$M = m_b 0.005 \frac{\rho_w c_{pw}}{L_i \rho_i \gamma_T} |(T^{3D}_{ocean} - T_f)|(T^{3D}_{ocean} - T_f) \quad (1)$$

where M is the melt rate in m/s, m_b is a scaling factor, ρ_w and ρ_i are ocean water and ice shelf density, respectively, c_{pw} is ocean water heat capacitiy, γ_T heat transfer coefficient, L_i latent heat, T_f freezing point at depth of ice and T^{3D}_{ocean} ambient ocean temperature. The ambient ocean temperature is derived from simple extrapolation of the 3D ocean temperature into the

P4, L32, calving parameterisations:
Are these two parameterisations (threshold and eigen) exclusive to each other?
If yes, then specify in the ensembles description that you explore the use of two different calving "laws", the threshold one with two values of its parameter and the eigen one with only one value.
If no, then please remove the eigen parameter value to the table summarizing the explored values of the parameters for the ensemble.

We rephrased the description of calving, hopefully clarifying that both parameterizations act simultaneously (p5, l12-17).

P5, l12-17

These scaling factors are kept constant throughout the paleo simulations. Ice shelf calving and therefore the dynamic calving front is derived via two heuristic calving parameterisations: 1. thickness calving (cH) sets a minimum spatially uniform ice thickness (75 m or 150 m) at the calving front, if the ice thickness drops below this threshold, ice in the respective grid node is purged; 2. independently of 1. we additionally employ Eigencalving (cE), which calculates a calving rate from the ice shelf strain rates (Albrecht and Levermann, 2014). Both calving parameterizations are active simultaneously throughout the simulations.

Table 2 shows the explored values of two parameters that are not described nor mentioned at all in the text: "sia" and "ssa". By looking at the values, I assume these refer to the enhancement factors of the SIA and the SSA parts of the simulated ice sheet. They need to be defined and properly named (sia and ssa are not parameters per se but approximations).

See changes applied to table 2 and caption table 2.

Table 2 shows the parameters till_min and till_max. These are not defined nor described in the text. The reader can only speculate about the possibility that these parameters have something to do with the description of page 3, last line: "[...] the yield stress (tau_c) is determined by the pore water content and the strength of the sediment which is set by a linear piecewise function dependent on the ice-bedrock interface depth relative to sea level". If the reader keeps digging and tries to identify these parameters in the references of the model given here, will still not succeed because no mention to "till_max" and "till_min" can be found in Bueler and Brown 2009, nor in Winkelmann et al, 2011. I had to go to Martien et al, 2011 (The Cryosphere) and assume that "till_min" and "till_max" correspond to the upper and lower numbers given by their equation 10. Is this correct?

Please define, clarify and cite accordingly.

The role of till_min and till_max was indeed not evident from the methods section, we added a short reference to the respective equation in Winkelmann et al 2011.

P4, l8-10

The relevant parameter for this approach is introduced in PISM via the till-friction angle (see Winkelmann et al. (2011) eq. 12) which is scaled linearly between $till_{min}$ and $till_{max}$, depending on the bedrock elevation.

1) Glacial index description.

Having the glacial index in Figure 5 and knowing that you use 3 climate snapshots weighted in time by such an index, one can have an idea of how you are forcing the ice sheet model.
However, the description of the method (including equations 1 to 5) is a bit odd. Perhaps it would be simply solved by providing the values of GI_pd and GI_max (as far as I saw the value of these parameters is not given in the manuscript).

We agree, that the description of the climate forcing should be expanded. To this end we introduce a plot which illustrates how the glacial index is implemented (p.7 new Figure 2). We also correct several typos in equations 5-7 (p6).

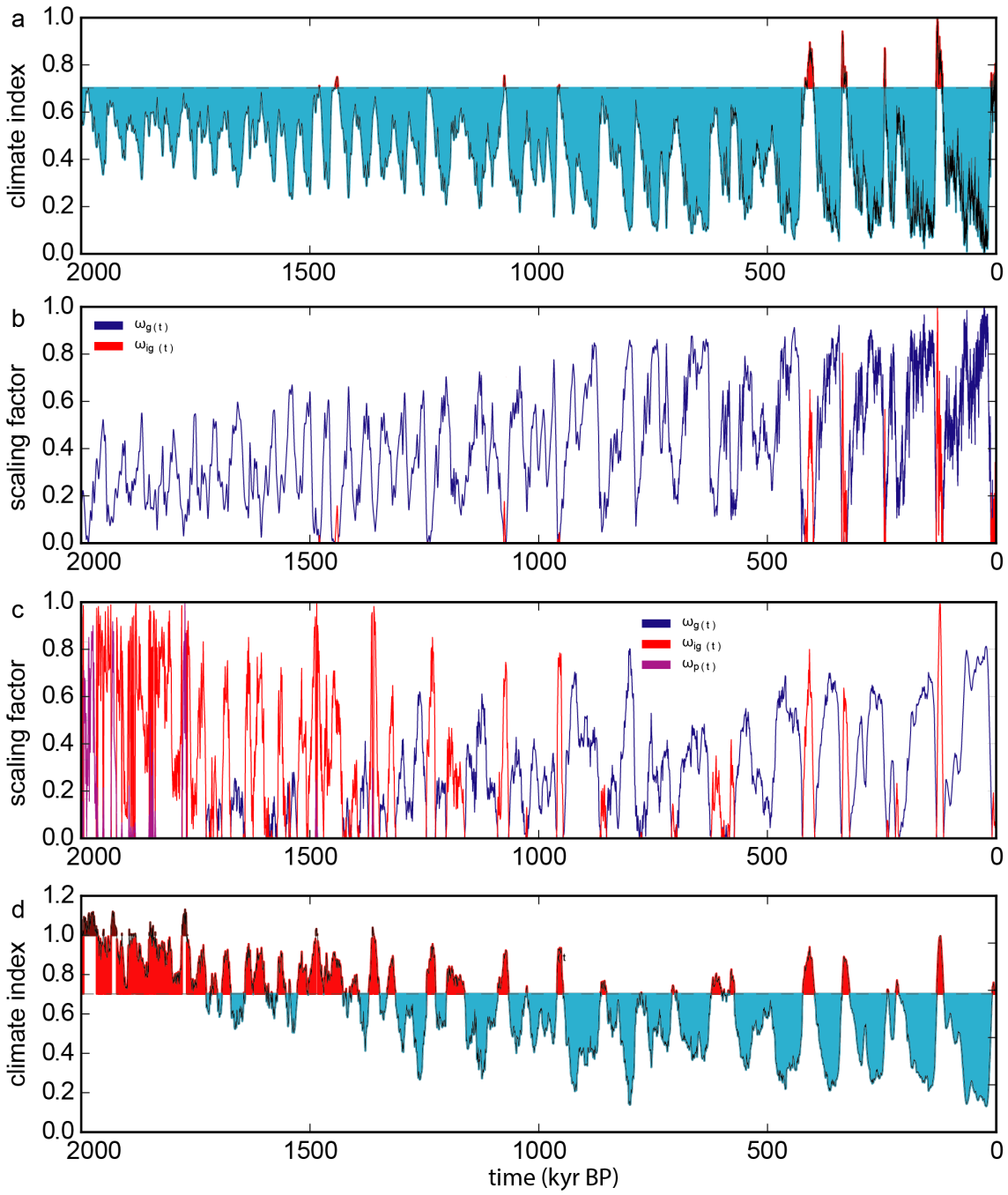

Figure 2. climate index derived from Dome C deuterium record a) and corresponding scaling factors ω_X in b). Times colder than present are shaded in cyan and times warmer than present in red. d) same as as a) but for climate index derived from the Snyder global surface temperature record and scaling factors ω_X in c) . Times warmer than the last Interglacial are shaded in dark red.

Otherwise the reader could wonder:

i) why is the value of the glacial index of ca. 0.7 during the Holocene? Does that mean you are taken a 30% of the LGM anomaly? (I guess not, and assume you put GI_pd to be approximately 0.7, so w_g in equation 3 goes to 0)

The climate index (called glacial index before, see ii)) is normalized with respect to the warmest climate period in the Dome C temperature record, therefore the LIG has index 1.0 in ensemble B1 and B2. The climate is linearly scaled between present day and LIG if the climate index surpasses the mean Holocene climate index which is ca. 0.7 (see inclusion starting on p6, l20).

P6, l20-

The respective values of the climate indices are CI_{lgm} = 0.0, CI_{pd} = 0.7022776, CI_{lig} = 1.0,CI_{p} = 1.130952. The climate index is normalized with respect to the warmest climate period in the Dome C temperature record, therefore the LIG has index 1.0 in ensemble B1 and B2. The climate is linearly scaled between present day and LIG if the climate index surpasses the mean present day climate index CI_{pd}, and between LIG and the Pliocene if the index is larger than 1.0.

ii) Is "glacial index" the right term for a curve that goes to 0 during glacial times? Would not be more appropriate to define it as (1-GI) or simply call it "climateindex"?

We agree that the term "glacial index" could lead to the impression that the index solely scales the climate between full glacial and present day conditions. We replace "glacial index" with "climate index" throughout the manuscript.

ii) What happens, for example when GI = 1.2 ? Do you take a linear interpolation of the Pliocene and the Last Interglacial climate fields? (I would assume so, because in equations 1 to 5 there is not any explicit differentiation of the time period, just a dependence on the values of the index, GI). If yes, can you justify it or elaborate?

Correct. Since the warmest climate period in the Snyder surface temperature record is not the LIG we interpolate between the LIG (climate index 1.0) and the warmest period in the Snyder climate index (ca. 1.2). Here, the climate is linearly scaled between peak LIG conditions (climate index 1.0) and peak climate conditions in the Pliocene (climate index ca 1.2).
The justification for the manner we implement the climate index is, that we assume, that qualitatively the climate system fluctuated throughout the Quaternary between interglacials and glacials as it did during the last glacial interglacial cycle. We are aware that this is a simplification, but we only had access to paleoclimate time slices from the LIG, LGM and Pliocene.

Furthermore, equation 6 must contain a typo or be wrongly formulated. In its current form, the more you cool from PD the more you increase the precipitation. Is that correct?

Typos / erratum on the glacial index description:
P5, L21: "T_opd is the surface temperature" (should be T_s)
P5, L22: commas missing after "LIG" and "LGM". I advise you to rephrase the whole sentence. P5, last line of equation 5: It reads "0.0 pdfor GI".

Corrected.

2) Other specific/technical comments:

P5, L2 reads. “To adequately capture continental ice sheet dynamics on long timescales (i.e. millennia and more), in principle, a coupled modelling approach is required to resolve climate-ice sheet interactions.”
I think I understand what you mean here, but I also believe a sentence that says “To capture A, a given approach is required to resolve B” does not make sense.

Agreed and changed.

P5, I 19-20

To adequately capture continental ice-sheet dynamics on multi-millenial timescales, in principle, a coupled modelling approach which resolves climate-ice-sheet interactions is required.

P9. L24: “The two clusters in the upper panel of Figure 5 show a present day ice sheet configuration (B1-branch) and a strong interglacial configuration in which the WAIS is collapsed (B2-branch)”.
I think this sentence needs some rephrasing.
By “.. show a present day and a strong interglacial” do you mean that their mean state is similar to the ones expected during present day and strong interglacial respectively?

Agreed and changed.

P12, l3-5

The two clusters in the upper panel of Figure 6 show an ice-sheet configuration similar to present day (B1-branch) and a strong interglacial configuration (B2-branch) in which the West Antarctic Ice Sheet (WAIS) has collapsed.

P9. L24: "...resembling the waxing and waning of the marine West Antarctic Ice Sheet"
"resembling" or "due to" the waxing and waning...?

Changed accordingly.

Figure 4: hard to see. Because not said in the caption, I assume black (or dark grey) thin lines in the top panel correspond to the individual realisations of the B1 ensemble. But, because the Pollard 2009, deBoer2014 and Tichgelaar 2018 curves are also plotted in dark grey or black they are really not distinguishable. Why not plotting the individual members in white or light grey as for the B2 ensemble?

Changed accordingly (now Figure 5).

At the end of section 3.1 you state: "[...] all simulations with the GHF field from Purucker (2013) exhibit a collapse of the WAIS in the LIG with a much smaller percentage for both Martos et al. (2017) and Shapiro and Ritzwoller (2004)."
Why is this? I see no obvious explanation since the West Antarctica GHF values from Purucker seem lower than those from Shapiro and way lower than Martos's.

Agreed. This sentence needs further explanation. However, we think that the role of geothermal heat flux on the stability of the WAIS and glaciers in general is a research field in its own right and therefore a detailed discussion would be beyond the scope of this manuscript. Regardless, we would like to keep the sentence in order to point out that GHF can have a decisive role for ice sheet systems which are close to a nonlinearity (i.e. MISI). We added a sentence, providing one potential reason for the outstanding effect of a very cold GHF underneath WAIS in Interglacials.

P16, l3-

All simulations with the GHF field from Purucker (2013) exhibit a collapse of the WAIS in the LIG with a much smaller percentage of simulations for both Martos et al. (2017) and Shapiro and Ritzwoller (2004). A thorough analysis of this result is beyond the scope of this manuscript, but it could be caused by larger glacial ice cover caused by the cold Purucker (2013) basal conditions. This would lead to an over-deepened bedrock and larger surface gradients along the coast at the onset of interglacials and therefore favourable conditions for the marine ice sheet instability.

Figure 6 left panel:
i) Are the LGM (and LIG) values given in red and blue the mean of the three particular cases shown in figure 5?
Please specify in the caption.
ii) If yes, why is the LGM mean (-6.12 m) considerably higher than the red (-9.65 m) and the blue (-10.17 m) means?
Is it because the red and blue values are simply the mean of the three particular cases and not the mean of the whole B1 and B2 ensembles?
If yes, what makes these 3 particular cases to show a bigger ice sheet than their respective sub-ensembles during the LGM?

If yes, can we learn something from this related to the conclusions of the paper?

Figure 6 middle and right panels:

- To what particular realisations of the ensemble do the 2D plots correspond to?
- Following the PD grounding line position line, I recognize indeed its current grounding line position but also its current ice front. Is that correct? Are you plotting both? If so, I would change the legend or specify it in the caption
- Why is the LGM grounding line of the Ronne ice shelf, Pine Island and west of the Antarctic Peninsula much more retreated than the one suggested by Bentley?
- Is this a result of the particular model realization or proper to the ensemble?

Figure 6:
It would be nice to have a third 2D panel showing the simulated PD ice sheet for the same parameters as for the LIG and LGM plots.

Caption of figure 6 reads: “Middel and left panel illustrate simulated ice sheet configurations for the LGM and Last Interglacial”.

Figure 6 is now split into two figures (Figure 7 on p14) and Figure 8 on p15. We hope Figure 8 provides an improved visual aid to the spread of the ensemble, with the main 8 ensemble members highlighted in colour for both B1 and B2.

We also add a discussion of the LGM grounding line position and the spread of results regarding LGM sea level contribution in Figure 8 (formerly Figure 6).

P14, l29 -

In general, the glacial extent of the AIS matches reconstructed LGM grounding margins rather well, with the notable exception of the Ammundsen and Bellinghausen sea sectors. In this region, the ocean forcing seems to be too warm to allow for an advance of the ice margin to the continental shelf edge in the model. LGM ice growth in the whole ensemble is strongly dependent on the SIA enhancement factor sia_e, with values larger than 1.5 leading to a underestimation of ice thickness, albeit not necessarily ice extent. In the Ross Sea, ice thickness calving exerts a strong influence on grounding line advance. A calving thickness of 75 generally leads to a good representation of LGM ice margin reconstructions (Bentley et al., 2014), while simulations with a thickness limit of 150m underestimate Ross Sea LGM grounding line advance. Furthermore, the parameterisation of ice shelf calving can play a preeminent role in interglacials, which underlines the dire need for a physical rather than heuristic representation of calving in ice-sheet models.

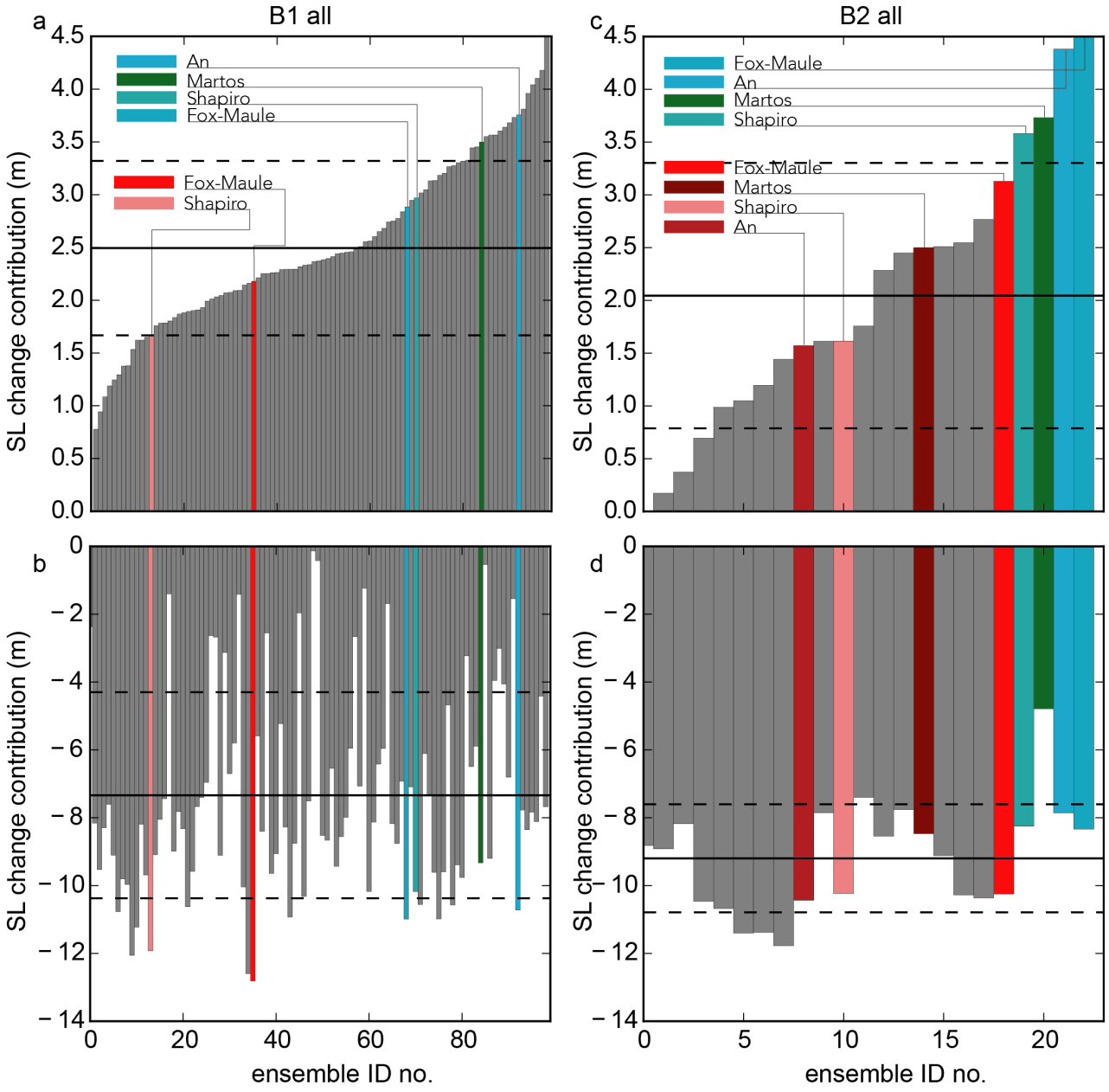

Figure 8. Sea level contribution in the LIG (a/b) and LGM (c/d) for the full ensemble forced with climate index B1 and climate index B2. The ensemble members focused on in this paper are highlighted with colours (P1 red colors, P2 blue/green colors). Horizontal black line depicts the full ensemble mean and the dashed line the standard deviation.

We expanded Figure 7, to illustrate the effects of the different forcing approaches on the spatial configuration of the AIS during the LIG, LGM and PD.

“Middel” is wronlgy spelled.
“Left” should be right. And invert the order of LGM and Last Interglacial.

Addressed (see new Figure 7).

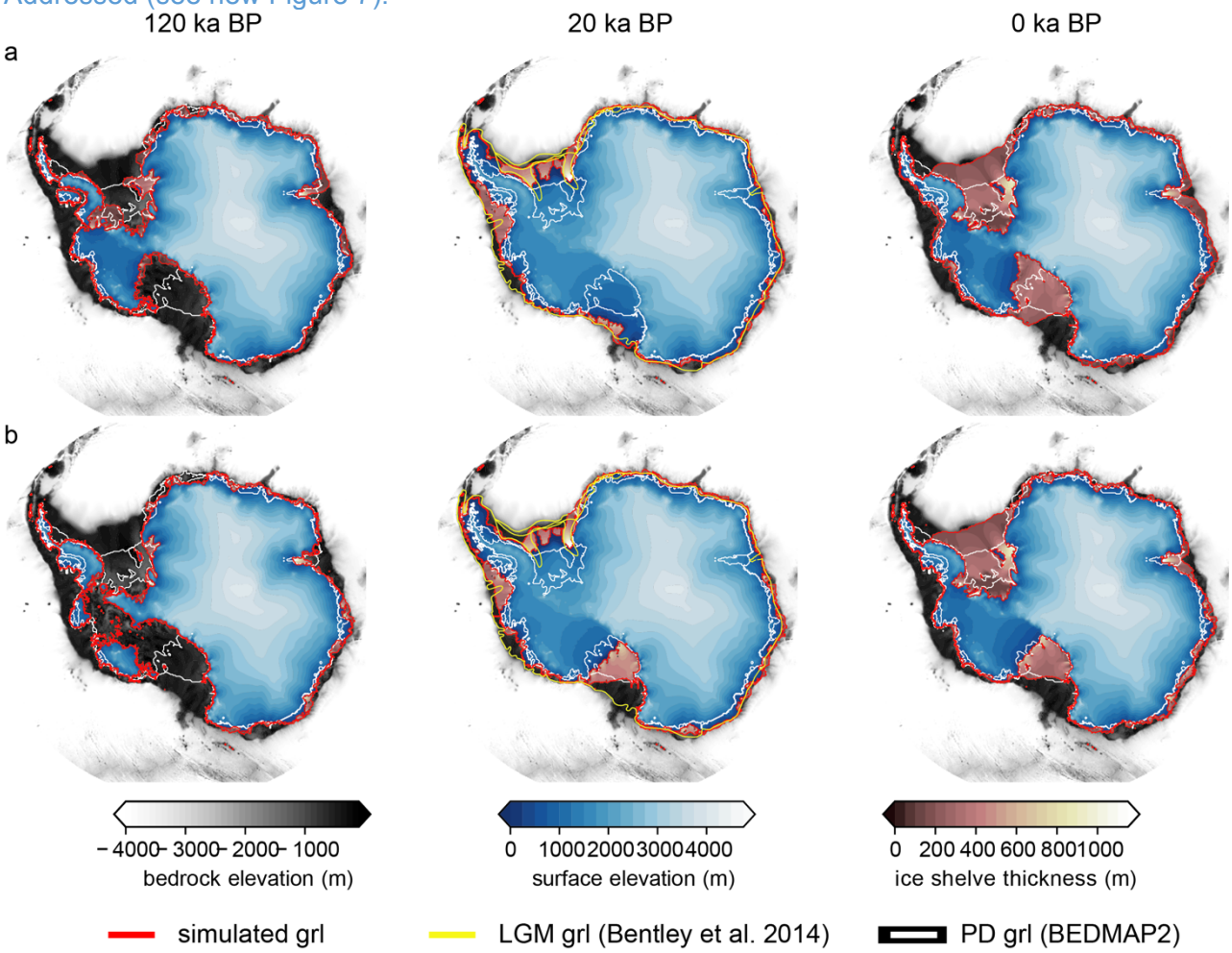

Figure 7. Panel a/b illustrate simulated ice-sheet configurations for the LIG, LGM and PD, respectively. Both simulations are carried out with forcing B1, using a different ice thickness calving limit (a: cH=75 m, b: cH=150 m). Reconstructed grounding line positions for the LGM (Bentley et al., 2014) are depicted in yellow, and both grounding line and ice shelf front from BEDMAP2 (Fretwell et al., 2013) are depicted in white.

P15, L6 reads: “Mean ice thickness variability for Dome Fuji and Dome C during the late Quaternary is 165 and 195 m, respectively (105 and 140 during pre-MPT).”
How is this “mean ice thickness variability” calculated? Is it the temporal standard deviation of the mean evolution of the ensemble, or has it something to do with the standard deviation of the ensemble itself?

Corrected. The increase is in mean ice thickness, not in variability. We added a sentence, pointing out the change in ice thickness variability (std) before and after the MPT.

Changes in the EAIS manifest in an increase in ice thickness by ca. 30% (mean ice thickness at ice core locations calculated for pre-MPT (1.8-1.2 Myr BP) and Quaternary (0.8-0.0 Myr BP)) time intervals alongside an increase in variability (standard deviation of ice thickness of individual ensemble members) of ca 50%.

P15, L7 reads: "Overall, the simulated present day ice cover after 2 million years at the highlighted ice core locations is in good agreement (within ≈ 5%) with the BEDMAP2 (Fretwell et al., 2013) data set."

This sentence does not seem precise enough. Does "present day ice cover" mean ice thickness? Here it is important to be precise, because it is not the same saying that the the error of the simulated region of Antarctica covered by ice falls within 5% with respect to BEDMAP2 than saying that the simulated thicknesses are within 5%. If the latter is what you meant, how did you calculate it?

We agree that this sentences requires clarification. We now specifically address the discrepancy of ice thickness at selected East Antarctic ice core locations (see below)

Somehow related: Why is Talos systematically too thin?

We agree that the TALDICE region ice thickness is not as well captured as for the other deep ice cores discussed here. We now address this discrepancy explicitly in the manuscript.

P19, l7-16

Overall, the simulated present day ice thickness after 2 million years at the highlighted ice core locations in East Antarctica is in good agreement with the ice thickness derived from the BEDMAP2 (Fretwell et al., 2013) data set (within ≈ 5% discrepancy in ice thickness for the selected ensemble members in B1 and B2). A notable exception is the Talos Dome ice thickness, which is too thin in all discussed B1 and B2 ensemble members except for the runs simulated with the relatively cold (Purucker 2013) and intermediate (Shapiro and Ritzwoller, 2004) GHF data set. The applied model resolution of 16km is generally to coarse to to accurately reconstruct smaller outlet glaciers and therefore might overestimate advection away from coastal ice domes.

P15, L11 reads: "We apply the conditions for the existence of 1.5 Myr old ice derived in Fischer et al. (2013) to our simulations …".
Please specify the conditions you refer to here. This would allow the reader to have an idea of your "oldest ice" results without having to look for such conditions in Fischer et al. 2013.

Agreed, we added the conditions for Oldest Ice from Fischer et al. 2013

P19, l6-9

We apply the conditions for the existence of 1.5 Myr old ice derived in Fischer et al. (2013) (ice thickness larger than 2000 m, basal melting zero and surface ice velocity slower than 1 m/a) […]

As a conclusion, I think this is a nice paper and that these comments represent only a minor revision, but I also fear that, in its current form, the reader would not appreciate the manuscript as much as they should. Therefore, I recommend the authors to correct all these minor issues and carefully go through the new manuscript in order to maximize reproducibility and a nice “flow” when reading it.

We thank Jorge Alvarez-Solas for his positive review of our manuscript and hope that the revised manuscript satisfactorily addresses all critical points.

We thank Bas de Boer for his thorough review on our paper and for his constructive comments and remarks. We hope that we were able to address them in a satisfactory manner and discuss the modifications we introduced motivated by the main remarks below. Please find all changes and the new or modified figures in the attached manuscript tracked in red. We also included the main changes below each comment in this document (response to reviewer comments in blue, changes to the manuscript in red).

1. Transfer function

As pointed out on line 15, page 5, you have used a transfer function to describe 2 Myr of climate variability, combining the EDC ice core record and LR04 benthic oxygen isotope stack. Please use a couple of sentences to describe this function in the main text.

This information was indeed missing and we now include a short description including the transfer function used (p5 l27-32).

and Raymo (2005) (LR04) or the global surface temperature data set from Snyder (2016). To obtain an "Antarctic" surface temperature record from the far field benthic oxygen isotope stack, the LR04 isotope values are scaled via:

$$LR04_T = -(LR04 - \overline{LR04_{810}})\frac{\sigma(EDC2007)}{\sigma(LR04_{810})} + \overline{EDC2007} - 55 \quad (1)$$

($LR04_T$) is the new surface temperature record, $LR04$ is the benthic isotope stack data (time corrected to match the AICC2012 time scale (Bazin et al., 2013; Veres et al., 2013)) and $\overline{LR04_{810}}$ the mean LR04 isotope data for the last 810 kyr, standard deviations of the EDC and $LR04_{810}$ record denoted by $\sigma(EDC2007)$ and $\sigma(LR04_{810})$, mean Dome C surface temperature record is denoted by $\overline{EDC2007}$. The forcing variables (surface temperature T_s, ocean temperature T_o) can then be calculated

2. Description of temperature forcing (eqns. 1 and 2)

The description of the temperature forcing in equations (1) and (2) should be expanded a bit more and made clearer. For example, since you use the temperatures at the LIG, LGM and Pliocene as anomalies, use a _T in the equations and description of the variables in the text below. Also describe all three anomalies below the equation for both surface and ocean temperatures as (for example):
"The ESM anomalies _Ts ig, _Ts g, and _Ts p, represent the LIG, LGM and Pliocene, respectively. Ocean temperatures (eqn. (2)) are defined in the same way."
Secondly, when describing the calculation of the weighting factor w, using the glacial indices, it is unclear how you distinguish between the three states (w_g, w_{ig} and w_p). Also, it would be good to have a Figure 2 close by to refer to the GI values over time (instead of places in Figure 5 only). Also, what are the values of GI_{PD} and GI_{max}? Do these vary between the two GI records? Also, why did you not shifted the index to have GI_{PD} = 1 or 0 for example? (since it is an index and can be shifted any way you want, as long as you coherently adapt equations 3-5). I do understand that since you have two GI records, based on Snyder and ice-core/_^{18}O records, the differences between the two need to stay intact.

We agree, that the description of the climate forcing should be expanded. To this end we introduce a plot which illustrates how the glacial index is implemented (p.7 new Figure 2). We also correct a mistake in equations 4-6 (p6).

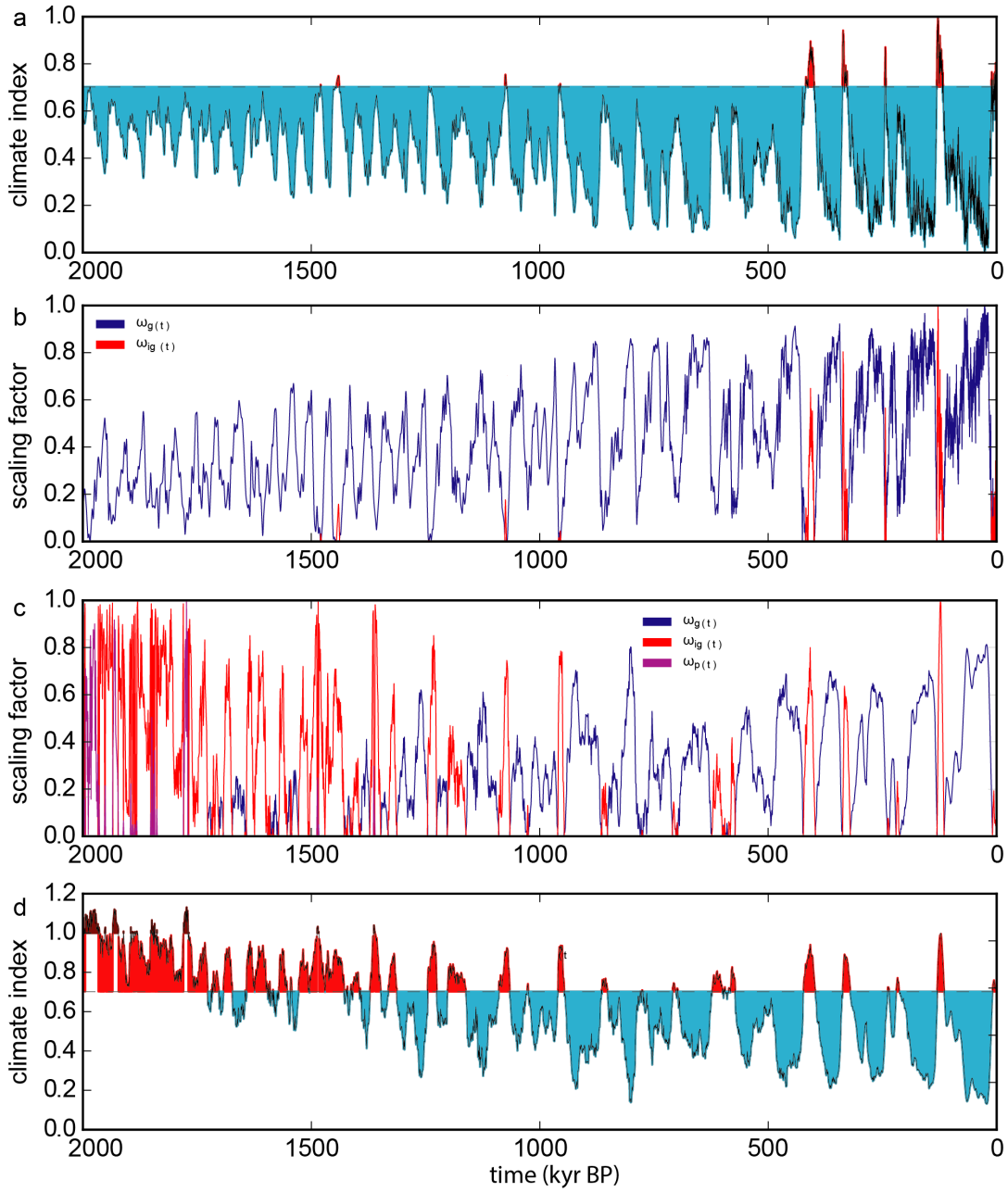

Figure 2. climate index derived from Dome C deuterium record a) and corresponding scaling factors ω_X in b). Times colder than present are shaded in cyan and times warmer than present in red. d) same as as a) but for climate index derived from the Snyder global air temperature record and scaling factors ω_X in c) . Times warmer than the last Interglacial are shaded in dark red.

3. Comparison with PD09 and dB14

As mentioned on line 3, page 10, you shortly explain the type of forcing used in the two other studies. For a good comparison I do think you have to add a bit more explanation on how these two studies derived a transient climate forcing, and use this later

on in your discussion as well. Both studies derive their long-term forcing in temperature and sea level from the LR04 benthic _^{18}O record, although applied in different ways. Also, they both use a weighting index (eqn 6 in PD09, equation 7 in dB14) to prescribe the variation in sub-oceanic melting. This weighting index includes solar variations (through an anomaly at 80S) which mainly controls the waxing and waning of the WAIS (see dB14 supplement figure S4). The large peaks towards lower ice volume are caused by including this insolation anomaly, so take this into account in your comparison/discussion. For more description of the methods, please see Methods section at the end of both papers.
Some more thoughts: It is a bit hard to distinguish individual simulations in Figure 5, but I guess your simulations of the B1-ensemble should be, in terms of timing, compare rather well to both PD09 and dB14 (depending on the sea-level forcing used). As you noted on line 6, page 10.

We agree, that the reader should be able to grasp major differences between the different studies approaches without doing a literature search first. We include a more detailed discussion of the approach in dB14 and P09 and a quick comparison of the main differences in the forcing approach with our study. We put the focus on basal shelf melt as we deem this to be the major difference affecting the simulated ice volume between the studies (p11 l 9-15, p12 l 1-2 & l 5-8.)

One of the main differences in the approach here and the forcing applied in Pollard and DeConto (2009) and de Boer et al. (2014), is the handling of basal melting underneath the ice shelves. This forcing component arguably exerts the strongest influence on grounding line migration of the AIS in interglacials. Our calculation of basal melt rates is very similar to de Boer et al. (2014), with lower differences between assumed peak interglacial and present day uniform ocean temperature. Peak interglacial temperature for ensemble B1 is approximately 2°C warmer than present day and 3°C warmer in B2 (3.7°C in de Boer et al (2014), -1.7°C at present day and +2°C at peak interglacial). Additionally, we increase the sensitivity of the basal melt rate to ocean temperature changes in certain ocean basins (see method section). Pollard and DeConto (2009) prescribe basal melt rates directly, scaling them via the far field benthic isotope record (Lisiecki and Raymo, 2005) and austral summer insolation. Ultimately this scaling leads to larger bulk ice shelf melt rates and smaller melt rates close to the grounding line compared to the ones calculated in our approach.

4. Structure of the ensemble

Based on the variables in Tables 1 and 2 you have a possible ensemble of 12 x 92 members. Please clarify in Section 2.3 how the two ensemble branches are built up. How many members does each have, and which specific experiments did you perform. All possible combinations? Or only a set? Also, in Table 2 the variable cE has only 1 value, so not a variable that you vary within the ensemble? If so, please remove form the table. What are the other settings of the model? Do you intend to include a parameter table? Or are these settings similar to previous simulations with PISM (please refer)?

This is indeed confusingly presented in the manuscript. We now address specifically which ensemble members are mainly analysed in the study (p8, l 8-10 & p9, l 1-4) and changed table 2 (p9) accordingly. Table 2 now provides the two main parameter sets used for all sea level and geothermal heat flux combinations in ensemble B1 and for all geothermal heat flux combinations in B2. We further provide additional parameter combinations simulated in the ensemble but not discussed in the manuscript in the third line of table 2. We hope this clarifies the main scope of the ensemble.

The constituting forcing set for the ensemble consists of four different geothermal heat flux and three sea level data sets, i.e. twelve individual experimental settings. We explore two main parameter sets (P1 and P2) highlighted in table 2. While we do take into account all sea level variations for ensemble B1 (48 individual experiments), we only look at the sea level forcing derived from Lisiecki and Raymo (2005) (LR05) in ensemble B2. We also experimented with other parameter choices based on table 2 (VP) but do cover all individual forcing sets, thus these are not discussed in this study. The ensemble

members discussed in this manuscript consist of 8 experiments for each ensemble B1 and B2 with sea level forcing from LR05.

Table 2. Selected ISM parameters for the model ensemble. First and second line show the main parameter sets used in the ensemble (P1 and P2). The third line lists additional parameters tested but not further explored (VP). cH stands for thickness calving limit (in meter), cE is a parameter in the Eigencalving equation. sia_e and ssa_e stand for the so called sia and ssa "enhancement factors", $till_{min}$ and $till_{max}$ modify basal friction in the sliding law. γ_{EAIS} is a dimensionless scaling factor for basal shelf melt for selected East Antarctic ice shelf regions (George V Land, Wilkes Land).

Parameter	sia_e	ssa_e	cH (m)	cE	$till_{min}$	$till_{max}$	γ_{EAIS}
P1	1.0	0.55	**75**	$1 \cdot 10^{17}$	5	30	**10**
P2	1.0	0.55	**150**	$1 \cdot 10^{17}$	5	30	**1**
VP	1.6 ; 1.7 ; 2.0	1.0	100	$1 \cdot 10^{18}$	10	40	5-20

5. Revise Figure 6

In general, I think your figures look really good. I do suggest you add panel labels to all figures (a,b,c, etc.) and use these in the captions. However, the left panel of figure C4 6 is unclear, and I cannot distinguish between the dots or triangles at all. I suggest you create a separate figure from the left panel and the two other panels (the maps). In the new figure 6, make the symbols much bigger and perhaps put the time frames next to each other (LGM, LIG and you could also add the simulated PreInd or PD ice volumes in the middle perhaps?). Please also mention the total number of simulations shown in the plot. Nice to add the values, that should be included again.
In the two panels with the map, please indicate which specific simulations you have used here. Is this a minimum/maximum within the ensemble, or a (sort of) reference simulation that represents the middle/median of the ensemble? Are the lines of LGM, PD and LIG shown in both panels?

Figure 6 is now split into two figures (Figure 7 on p14 and Figure 8 on p15). We hope Figure 8 provides an improved visual aid to the spread of the ensemble, with the main 8 ensemble members highlighted in colour for both B1 and B2.

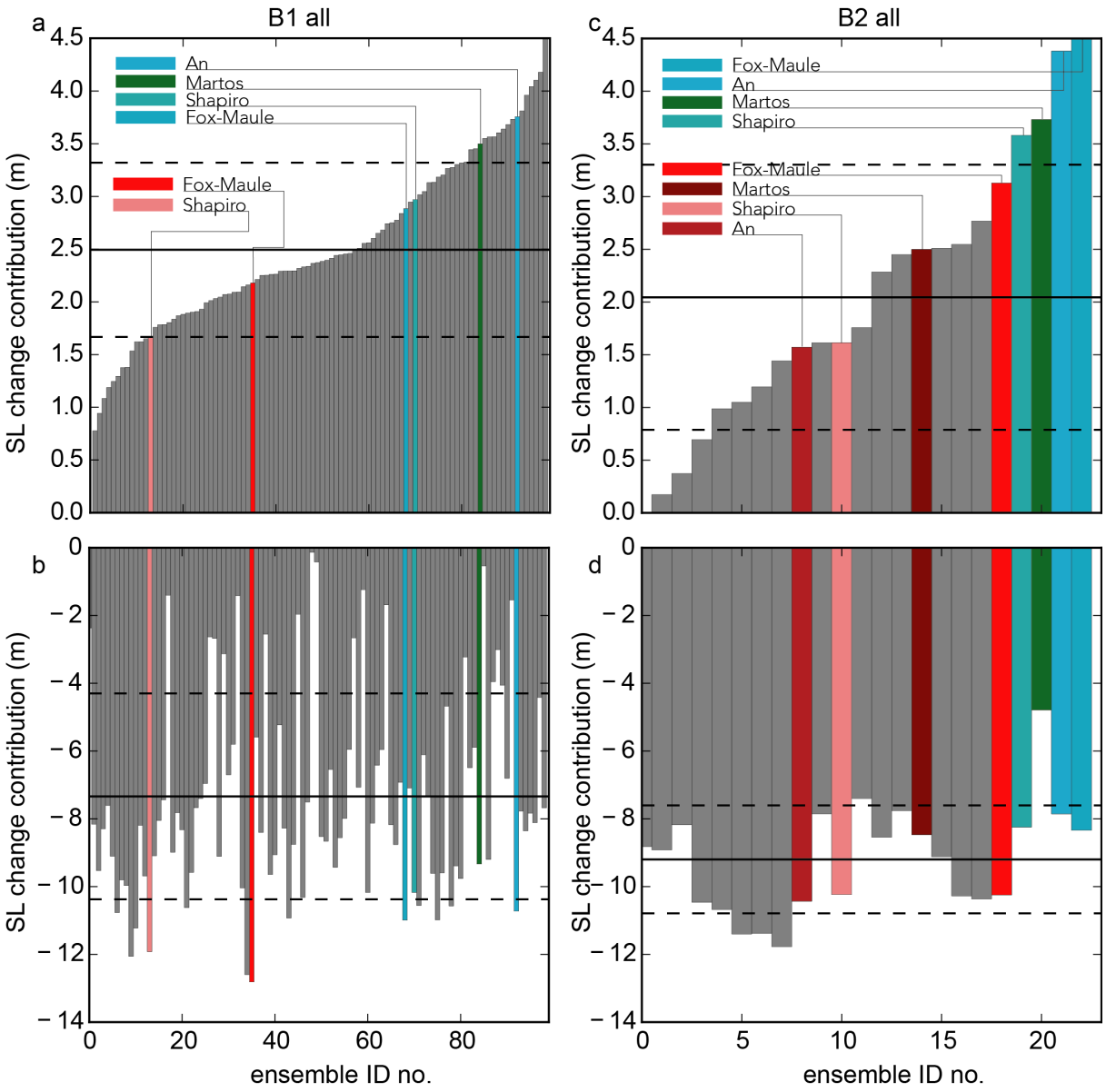

Figure 8. Sea level contribution in the LIG (a/b) and LGM (c/d) for the full ensemble forced with climate index B1 and climate index B2. The ensemble members focused on in this paper are highlighted with colours (P1 red colors, P2 blue/green colors). Horizontal black line depicts the full ensemble mean and the dashed line the standard deviation.

We expanded Figure 7, to illustrate the effects of the different forcing approaches on the spatial configuration of the AIS during the LIG, LGM and PD.

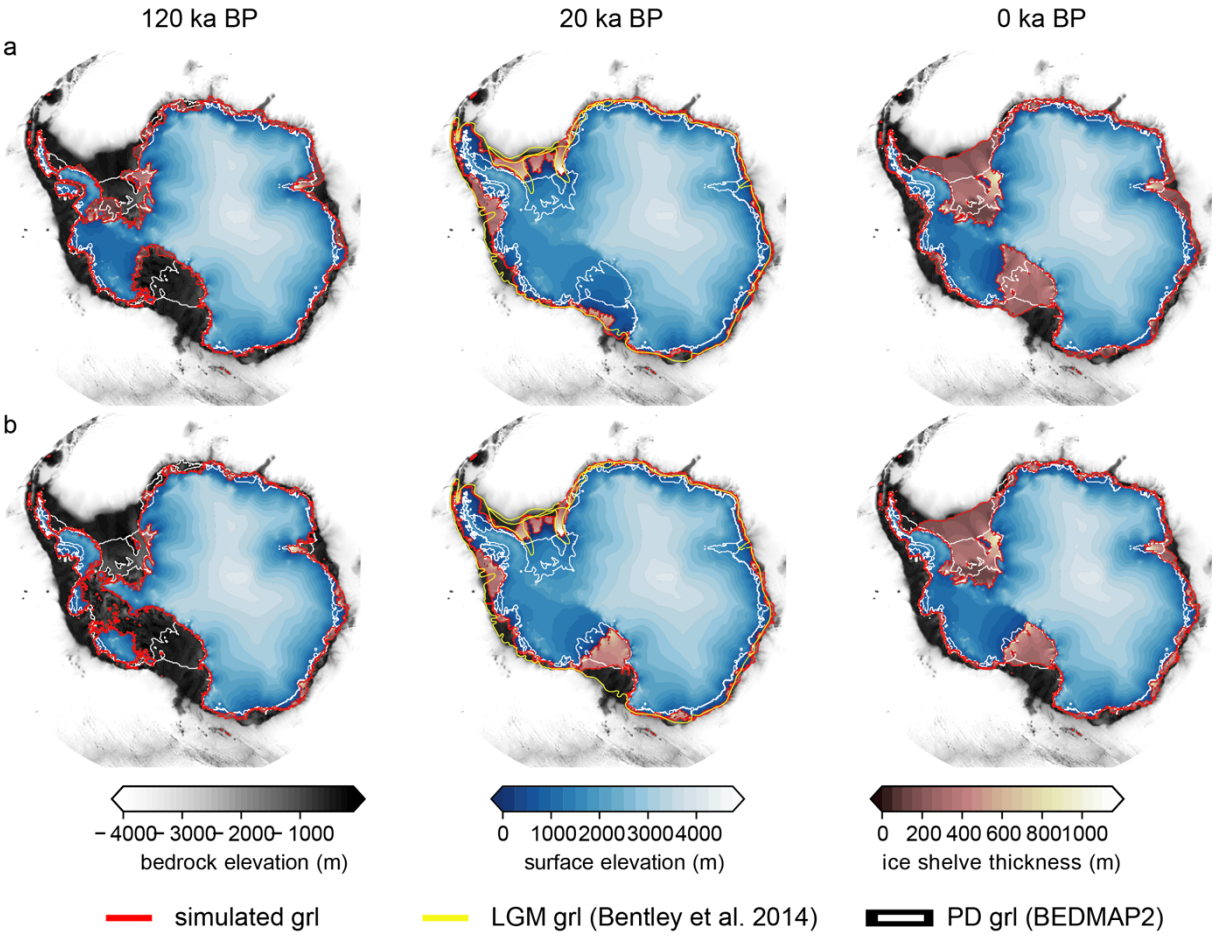

Figure 7. Panel a/b illustrate simulated ice-sheet configurations for the LIG, LGM and PD, respectively. Both simulations are carried out with forcing B1, using a different ice thickness calving limit (a: cH=75 m, b: cH=150 m). Reconstructed grounding line positions for the LGM (Bentley et al., 2014) are depicted in yellow, and both grounding line and ice shelf front from BEDMAP2 (Fretwell et al., 2013) are depicted in white.

6. Revise Figure 9

Also, figure 9 is not really clear for me, took quite some time to get the full picture right. Please indicate for each panel what it shows, i.e. write type of experiment above the labels or ordered in a 4x4 grid. Make the lines of the ice divides thicker. Since you have so many panels, I don't think panel labels are useful here. What is the purpose of the big central panel, just as an overview? It takes away the attention so if it is less important, position it more on the side. Also, make a clearer division between the different sensitivity experiments with using names on top of the figures and put the colour bars at the bottom of the figure. Something like a 4x4 panel, with the x-axis (on top) the four different regions and the y-axis (on the left) the four different GHF datasets used. And then the big panel on the left.

We modified Figure 9 (now Figure 11p19) as suggested.

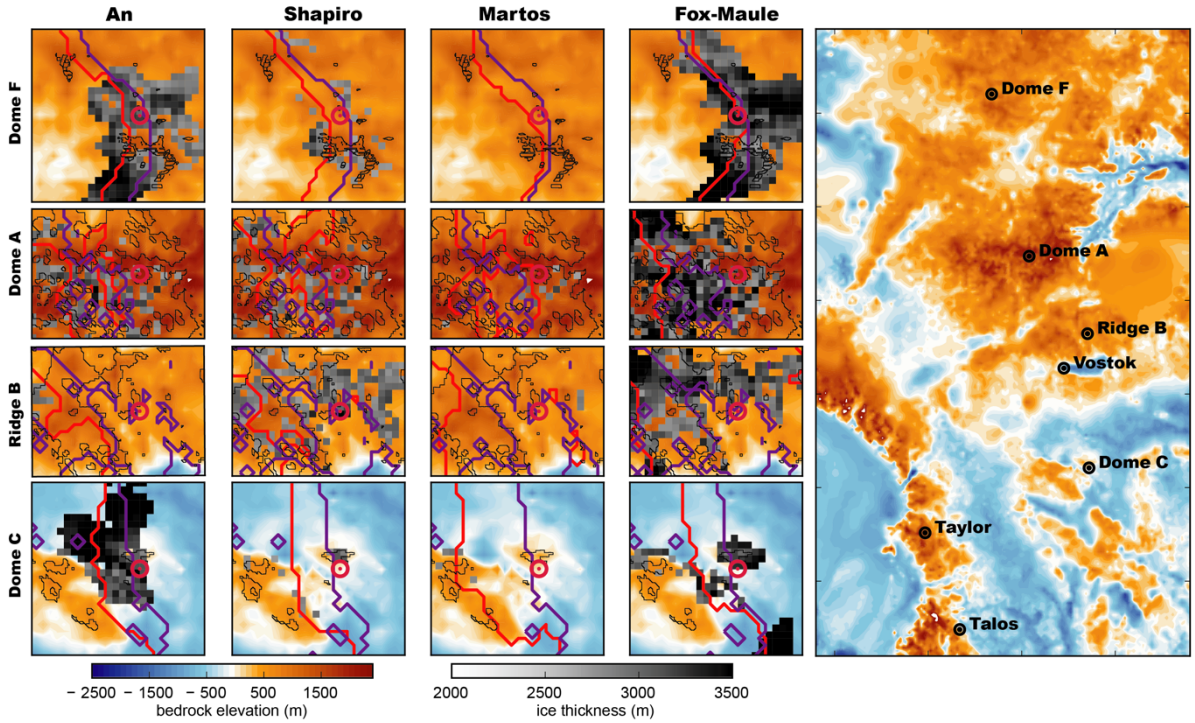

Figure 11. Comparison between regions of Oldest Ice identified in this study and in Van Liefferinge and Pattyn (2013) (Ridge B, Dome A) and Van Liefferinge et al. (2018) (Dome C, Dome Fuji) outlined in black. Regions of oldest ice are defined as grid nodes where ice thickness is larger than 2000 m, basal melting is zero and surface ice velocity slower than 1 m/a (boxes coloured in grayscale). The left matrix columns show magnified sections centred at Dome Fuji, Ridge B and Dome C for identical parameter sets and forcing but different geothermal heat flux (from left An et al. (2015), Shapiro and Ritzwoller (2004), Martos et al. (2017) and Purucker (2013) GHF forcing). The red line in blown up regions depicts simulated present day ice divide (defined as position where surface elevation gradient switches sign), while the dark rose line depicts the present day ice divide as computed from BEDMAP2.

7. Reference list
I have added some minor comments in the reference list, seems to have some issues with the copy from Bibtex (in case you have used latex). Please carefully check your list of references on errors in mainly page numbers and hyperlinks via doi.

This is now corrected.

We thank Bas de Boer for his positive review of our manuscript and hope that the revised manuscript satisfactorily addresses all critical points.